

**Experimental Investigation of Natural Convection from Pinned Plate Solar
Absorber**

by

Normanisah Binti Mat Ghani

Dissertation submitted in partial fulfilment of
the requirements for the
Bachelor of Engineering (Hons)
(Mechanical Engineering)

SEPTEMBER 2012

Universiti Teknologi PETRONAS
Bandar Seri Iskandar
31750 Tronoh
Perak Darul Ridzuan

CERTIFICATION OF APPROVAL

Experimental Investigation of Natural Convection from Pinned Plate Solar

Absorber

by

Normanisah Binti Mat Ghani

A project dissertation submitted to the
Mechanical Engineering Programme
Universiti Teknologi PETRONAS
in partial fulfillment of the requirement for the
BACHELOR OF ENGINEERING (Hons)
(MECHANICAL ENGINEERING)

Approved by,

(Assoc. Prof. Dr. Hussain H. Al-Kayiem)

UNIVERSITI TEKNOLOGI PETRONAS
TRONOH, PERAK
September 2012

CERTIFICATION OF ORIGINALITY

This is to certify that I am responsible for the work submitted in this project, that the original work is my own except as specified in the references and acknowledgements, and that the original work contained herein have not been undertaken or done by unspecified sources or persons.

NORMANISAH BINTI MAT GHANI

ABSTRACT

Experimental Investigation of Natural Convection Heat Transfer on Pinned Plate Solar Absorber

Solar collector consists of a solar absorber which absorbs heat from short wave solar radiation and transfers the heat to the working fluid for storage or use. Instead of merely a normal flat plate, staggered pinned plate absorbers with different surface roughness – 2 mm, 3mm and 4 mm height are introduced in this project. The main interest is on the effect of turbulence of absorber plates on the natural convection heat transfer process of the air heating solar collectors. The paper investigates the effect of inclination angle and absorber types on the heat transfer, solar insolation, air outlet temperature and velocity, etc. It involves series of experimental works conducted on 4 solar collector test rigs simultaneously that were ran at 10°, 30°, 50°, 70° and 90° inclination angles. For each configuration, the experiments are repeated for four consecutive days. Readings were recorded at two hours intervals from 8am until 6pm for data collection of the investigated parameters. Solar insolation is higher for system at lower inclination angle yet for convective heat transfer coefficient; it is optimum at 50° inclination angle which best at 45°. Solar collectors with pinned plate absorbers are noticeably provides better outlet temperature and heat transfer rate than a normal flat plate absorber where the 2mm is the best pursued by 3mm and 4mm pinned absorbers. The boundary layer is disturbed in channel with pinned plate thus the effect of added turbulent enhance the heat transfer. The overall system at all configurations possesses a mixed convection, turbulent flow behavior thus invalid the claims of natural convection.

ACKNOWLEDGEMENT

The special thank goes especially to my supervisor, Assoc. Prof. Dr. Hussain H. Al-Kayiem from Mechanical Engineering Department, Universiti Teknologi PETRONAS for giving me such opportunity to work under his supervision on “Experimental Investigation of Natural Convection from Pinned Plate Solar Absorber” project. The supervision, support and guide that he gave me throughout the completion of this final year project despite his hectic schedule are much indeed appreciated. Besides, I would also thank Miss Chin Yee Sing who also contributes to this project betterment.

I also wish to express my sincere gratitude to Mr. Tadahmun Ahmed Yassen, PhD. Research students from Mechanical Engineering Department, Universiti Teknologi PETRONAS who is like my second hand in completing this project. Without his assistance and guidance, it would be much difficult to complete the project particularly the experimental works smoothly. I would like to thank him and not to forget Mr. Aja Ogboo Chikere for their time and willingness to assist and guide me also for the encouragement they gave me throughout this project completion.

Besides, I also would like to thank my institution and my faculty members who had been directly and indirectly involved in this project. Lastly, I wish to express a sense of gratitude and love to my family especially Megat Faisal Hafni Rozli for great support and encouragement they gave me which boosting my motivation in completing this project.

TABLE OF CONTENTS

CERTIFICATION OF APPROVAL	i
CERTIFICATION OF ORIGINALITY	ii
ABSTRACT	iii
ACKNOWLEDGEMENT	iv
CHAPTER 1: INTRODUCTION	1
1.1 Background of Study	1
1.2 Problem Statements	4
1.3 Objectives	4
1.4 Scope of Study	4
1.5 Relevancy of the Project	5
1.6 Significance of the Project	5
1.7 Feasibility of the Project	6
CHAPTER 2: LITERATURE REVIEW	7
CHAPTER 3: METHODOLOGY	18
3.1 Research Methodology	18
3.2 Project Activities Flow Chart	20
3.3 Analytical Analysis	23
3.4 Key Milestones	23
3.5 Project Gantt Chart	24
3.6 Tools and Software	24
3.7 Experimental Setup	26

CHAPTER 4:	RESULTS AND DISCUSSION	.	.	.	29
CHAPTER 5:	CONCLUSION AND RECOMMENDATION	.			46
	5.1 Recommendations	.	.	.	47
	5.2 Relevancy to the Objectives	.	.	.	48
REFERENCES	49
APPENDICES	52
	APPENDIX I	RAW DATA	.	.	53
	APPENDIX II	ANALYZED DATA	.	.	58

LIST OF FIGURES

Figure 1.1	Illustration of solar chimney working principle	2
Figure 1.2	Illustration of Trombe Wall working principle	3
Figure 2.1	Pictorial view of a flat plate collector	8
Figure 2.2	Analysis model of solar collector subjected to solar and thermal irradiations	9
Figure 2.3	Horizontal rectangular enclosure	13
Figure 2.4	Inclined rectangular enclosure	14
Figure 2.5	Vertical rectangular enclosure	14
Figure 2.6:	a) In-Line or Parallel arrangement b) Staggered arrangement	17
Figure 2.7	Pin fin geometry	17
Figure 3.1	Geometry of staggered pinned plate	18
Figure 3.2	Physical model of double glazing solar collector	19
Figure 3.3	Project activities flow chart	20
Figure 3.4	Regime of free, forced and mixed convection for flow through vertical tubes according to Metais and Eckert	21
Figure 3.5	Regime of free, forced and mixed convection for flow through horizontal tubes according to Metais and Eckert	22
Figure 3.6	Test rigs at 10° inclination angle	26
Figure 3.7	Test rigs at 30° inclination angle	26
Figure 3.8	Test rigs at 50° inclination angle	27
Figure 3.9	Test rigs at 70° tilt angle	27

Figure 3.10	Test rigs at 90° tilt angle	27
Figure 3.11	Isometric view of the solar collector test rig	28
Figure 4.1	Insolation profile at different inclination angles	29
Figure 4.2	Outlet temperature profile for inclination angle at 08:00	31
Figure 4.3	Outlet temperature profile for inclination angle at 10:00	32
Figure 4.4	Outlet temperature profile for inclination angle at 12:00	32
Figure 4.5	Outlet temperature profile for inclination angle at 14:00	32
Figure 4.6	Outlet temperature profile for inclination angle at 16:00	33
Figure 4.7	Outlet temperature profile for inclination angle at 18:00	33
Figure 4.8	Convective heat transfer coefficient for 2mm pinned	35
Figure 4.9	Convective heat transfer coefficient for 3mm pinned	35
Figure 4.10	Convective heat transfer coefficient for 4mm pinned	35
Figure 4.11	Convective heat transfer coefficient for flat plate	36
Figure 4.12	Heat transfer rate for different absorber types at 10° tilt angle	37
Figure 4.13	Heat transfer rate for different absorber types at 30° tilt angle	37
Figure 4.14	Heat transfer rate for different absorber types at 50° tilt angle	37
Figure 4.15	Heat transfer rate for different absorber types at 70° tilt angle	38
Figure 4.16	Heat transfer rate for different absorber types at 90° tilt angle	38
Figure 4.17	Air outlet velocity profile for 10° inclination angle	39
Figure 4.18	Air outlet velocity profile for 30° inclination angle	39
Figure 4.19	Air outlet velocity profile for 50° inclination angle	39
Figure 4.20	Air outlet velocity profile for 70° inclination angle	39
Figure 4.21	Air outlet velocity profile for 90° inclination angle	40

Figure 4.22	Reynolds no. against time at 10° inclination angle	40
Figure 4.23	Reynolds no. against time at 30° inclination angle	41
Figure 4.24	Reynolds no. against time at 50° inclination angle	41
Figure 4.25	Reynolds no. against time at 70° inclination angle	41
Figure 4.26	Reynolds no. against time at 90° inclination angle	42
Figure 4.27	Relationship between Nu and Ra at 50° inclination angle	44

LIST OF TABLES

Table 2.1	Range of Prandtl number	11
Table 2.2	Critical angle for inclined rectangular cavities	13
Table 3.1	Timeline for each key milestone	23
Table 3.2	Final Year Project I Project Gantt chart	23
Table 3.3	Final Year Project II Project Gantt chart	24
Table 3.4	Software and their purposes	24
Table 3.5	Equipments and their purposes	25
Table 4.1	Solar insolation intensity at different inclination angle	29
Table 4.2	Air outlet temperature at different inclination angle	31
Table 4.3	Convective heat transfer coefficient	34
Table 4.4	Comparison on Nusselt number of different correlations at 12pm	44

NOMENCLATURES

\dot{Q}	rate of convective heat transfer (W)
h	convective heat transfer coefficient ($W/m^2 K$)
A_s	surface area, (m^2)
L_c	characteristic length of the geometry (m)
D_h	hydraulic diameter (m)
L	length of the rectangular duct (m)
W	width of the rectangular duct (m)
H	height of the rectangular duct (m)
T_f	film temperature ($^{\circ}C$)
T_1	temperature of hot surface (absorber), ($^{\circ}C$)
T_2	temperature of cold surface (glazing cover facing absorber), ($^{\circ}C$)
V	free stream velocity (m/s)
T_{G1}	temperature of outer glazing cover ($^{\circ}C$)
T_{G2}	temperature of inner glazing cover ($^{\circ}C$)
T_A	temperature of absorber plate ($^{\circ}C$)
T_{amb}	Ambient temperature ($^{\circ}C$)
T_{out}	outlet air temperature of the solar collector ($^{\circ}C$)
S	solar insolation (W/m^2)
V_{amb}	ambient wind speed (m/s)
V_{out}	air velocity at the channel outlet (m/s)

Dimensionless number

Pr	Prandtl number
Nu	Nusselt number
Ra	Rayleigh number
Re	Reynolds number
Gr	Grashof number
Gr_{cr}	Critical Grashof number
Gz	Graetz number

Properties of air

ν	kinematic viscosity (m^2/s)
α	thermal diffusivity (m^2/s)
μ	dynamic viscosity ($kg/m.s$)
μ_b	dynamic viscosity evaluated at bulk temperature ($kg/m.s$)
μ_w	dynamic viscosity evaluated at film temperature ($kg/m.s$)
C_p	specific heat of air ($J/kg.K$)
β	coefficient of thermal expansion ($1/K$)
g	gravitational acceleration (m/s^2)
k	thermal conductivity ($W/m.K$)
ρ	density of air (kg/m^3)
\dot{m}	mass flow rate of air inside channel (kg/s)

CHAPTER 1

INTRODUCTION

1.1 Background of Study

Today world main resources of energy supply, fossil fuel reserves are expected to deplete in about 35, 107 and 37 years time for oil, coal and gas respectively (Shafiee and Topal, 2008) ^[1]. Alternative energy, mainly the solar energy thus will play an important role in future energy supply, to the advantage of both the environment and the economy. Solar energy applications can be broadly classified into two main categories which are thermal systems and photovoltaic system. Solar thermal systems can either be the water or air based system depending on the heat transfer fluid utilized. This study simply focuses on the solar thermal system which converts solar energy to thermal energy with air as the working fluid. Photovoltaic systems in the other hand generate electricity from the solar energy absorbed.

According to Kalogirou ^[2], for every solar thermal system, the most important component is of course the solar collector which responsible for absorption of incoming solar insolation and transfers of the heat to the working fluid. Solar collectors available in various types including flat-plate, compound parabolic, evacuated tube, parabolic trough, Fresnel lens, parabolic dish and heliostat field collector. However, a flat plate solar collector is the common and most widely used for solar energy applications that required heat at temperature below 80°C. A typical flat plate solar collector normally consists of absorber plate, transparent glazing cover, thermal insulation, heat removal system, and the casing.

The basic theory behind the heat transfer on air solar collector is the natural convection. This heat transfer mode created by the buoyancy forces due to density of the air changes proportionally with variations in temperature. When the solar radiation from the Sun falls on the absorber plate inside the solar collector, large portion of this solar energy will be absorbed due to its high absorptivity and converted into heat energy. The heat energy is then transferred to the air inside the solar collector thus increasing the temperature. As temperature rise, the air expands

so its density becomes lighter and subsequently the less dense air naturally rises upward. The outside air which is cooler enters the solar collector to replace the rise air, will also be heated and rise continuously. The circulation of the air through this natural driven force makes up the functionality of the solar collector.

The most common applications of air heating solar collectors are solar chimney and Trombe Wall. **Figure 1.1** shows an illustration of solar chimney application for cooling and heating purposes. A solar chimney uses the natural convection of air heated by passive solar energy to improve the ventilation of buildings. Cooling effect as in solar chimney in Figure 1.1 can be created by opening the top exterior vents to allow warm air to rise by convection and escape to the outside. At the same time cooler air can be drawn in through vents at the lower level. For heating effect, the working principle is much similar to Trombe wall as the top exterior vents are closed but at the same time, high interior vents are opened. Since the top exterior vent are closed the heated air cannot escape through the top but the opened high interior vent let the heated air into occupied spaces providing convective air heating (Autodesk, 2011) ^[3].



Figure 1.1 Illustration of solar chimney working principle ^[3]

On the other hand Trombe wall as shown in **Figure 1.2** below is used to trap the passive solar energy to warm up the living room. During the day, sunlight shines through the glazing and hits the surface of the thick masonry wall (thermal mass), warming it by absorption. The heat collected from the sunlight is trapped between glazing and the thermal mass thus heated the air inside via heat conduction and rises, taking heat with it due to convection. The warmer air moves through the vents at the tops of the wall and into the living area while cool air from the living area enters the vents near the bottom of the wall. At night, a one-way flap on the bottom vents prevents the backflow, which could give undesired reverse cooling effect. In

addition, the heat stored in the thermal mass radiates into the living area to continuously warming the living space [4].

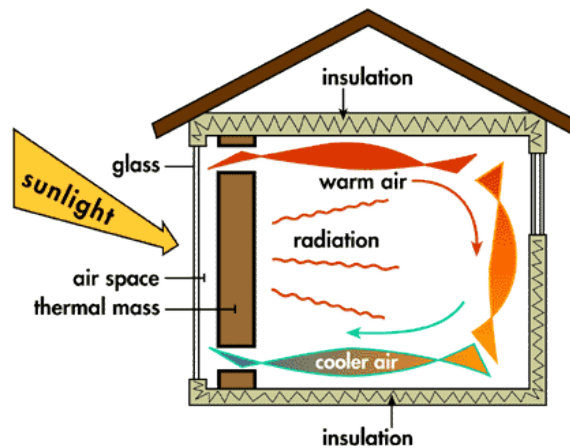


Figure 1.2 Illustration of Trombe wall working principle [4]

Besides that, air heating solar collector can also be used in heat process applications such as drying laundry, crops in agriculture, manufacturing process drying and other drying applications. Air heated through a solar collector and then passed over a medium to be dried can provide an efficient means by which reduce the moisture content of the material [5]. The applications of air heating solar collector becomes even wider nowadays thus enhance the importance of flat plate solar collector.

The development of solar collectors either air or water heating system has been intensive ever since the oil crises of the 1970s and over the years, extensive development work has been carried out to find efficient solar collector constructions (Lars Andrén, 2003) [6]. People have tried various means in increasing the efficiency of solar collector and normally focuses are on the types of materials used for each component of solar collector, the orientation (position) and tilt angle, the design parameters, geometry, moving sun tracking method and etc. As a new approach to improvise the flat plate solar collector, staggered pins will be introduced onto the absorber plate in this project as a trial to increase the heat transfer rate thus increase the efficiency of the solar collector. The pins as they offered a larger effective surface area for solar insolation absorption; it is possible to enhance the natural convection heat transfer rate of this thermal solar system. Transient heat transfer behaviour of laminar and turbulence flow of air above the absorber plate of the collector in the presence of the pins become another interest of this studies.

1.2 Problem Statements

A normal flat plate solar collector which is the most widely used air heating solar collector provides good enough heat transfer rate but research and development works never stop. The search for a better construction of flat plate solar collector which can offer higher efficiency led to the introduction of staggered pinned plate absorber in this project. Via experimental analysis, the relationship between the natural convection heat transfer rate due to different variables and various parameters such as the outlet temperature (thermal), solar insolation, the turbulence effect (fluid dynamic) of the system and etc are to be determined. The effect of inclination angle and types of absorber plates (pinned plate and flat plate) on the Nusselt number (Nu) and Reynolds number (Re) are also another interest of this project.

1.3 Objectives

The main aim of this project is to investigate the effect of the absorber plate's turbulation on heat transfer process and relate it with various parameters such as outlet temperature, solar insolation, air velocity inside the channel and etc. In order to investigate their relationship, several variables have been introduced in this project which is explained in the next section.

1.4 Scope of Study

This project involved series of both technical and experimental works. Some technical works are performed to prepare the absorber plates with different surface roughness – flat and pinned. The pins with different height (2mm, 3 mm, and 4mm) are punched in staggered onto the aluminium absorber plates of 2m length. The solar collector test rigs also being prepared for the experimental works which are drawn based on following targets:

- i. To study the effect of different **inclination angle** on the outlet temperature of the pinned plate solar collector and insolation at various time

- ii. To investigate the effect of different **height of the pins** or **types of absorber plates** on heat transfer and air flow behaviour or the turbulence effect.
- iii. To compare between **staggered pinned plate solar collector** and the **normal flat plate** solar collector on various parameters

The collected data from the experiments are analyzed and comparison between the pinned plates and typical flat plate solar absorber of the air heating solar collector on the natural convection heat transfer and other parameters are made. Some of the data are validated through various convection heat transfer correlations.

1.5 Relevancy of the Project

The experiment is conducted in University Technology of PETRONAS (UTP) solar research site (SRS) where the average normal temperature is about 30 °C. It can be considered as quite ‘hot’ with high intensity of solar insolation, thus very suitable for solar collector application. The investigation on the flat plate solar collector has been carried out before at the same place thus makes it very practical for comparison with this experiment. From this experimental analysis, the thermal and fluid dynamic behaviour of the system can be determined thus able to investigate whether pinned plate solar collector is better than flat plate solar collector in term of heat transfer rate and efficiency in extracting the solar energy from the sun radiation.

1.6 Significance of the Project

This experimental investigation is significant in a way that it provides some alternatives in enhancing the efficiency of a normal solar collector. The results of this experiment could determine either the staggered pinned absorber is better than a normal flat plate solar absorber in term of natural convection heat transfer rate and other criteria. This information would be very useful for the engineers or solar collector investigator to improve the design of the conventional solar collector to the desired standards and specification for industrial applications.

1.7 Feasibility of the Project within Time Frame and Scope

The time allocated for completing the whole project requirement is two semesters which is about 28 weeks in total. The first semester is allocated for the project research and fabrication of the test rig, thus within 14 weeks the project is very feasible with the time frame. While the experimental works which required about 20 days of experimental work for data collection, is also feasible within the time frame. The application and integration of knowledge learnt from Alternative Energy course enhances the understanding on this project.

CHAPTER 2

LITERATURE REVIEW

The ultimate source of solar energy, Sun which provides heat, light and energy to all living things in the Earth is the most inexhaustible, renewable source of energy known to man. The Sun delivers about 7000 times more energy to the Earth's surface than the current demand for global consumption as for every 15 minutes; the Sun produces enough power to supply the earth for an entire year. Even if small portion of this massive solar energy can be extracted, it could reduce human dependence on the fossil fuel (Nielsen, 2005) ^[7]. Extraction of the solar energy directly to electricity can be done through photovoltaic cells while conversion of solar energy to thermal or heat energy can be generated through the solar thermal system.

Solar collectors; the major component of a solar thermal system can be classified into two types distinguished by their motion: non-concentrating or stationary and concentrating. A non-concentrating collector has the same area for intercepting and absorbing solar radiation, whereas a sun-tracking concentrating solar collector usually has concave reflecting surfaces to intercept and focus the sun's beam radiation to a smaller receiving area, thereby increasing the radiation flux (Kalogirou, 2004) ^[2]. Among the three types of collectors fall in this stationary category, flat plate solar collector is most common solar collector used instead of evacuated tube collector and stationary compound parabolic collector. The basic components of a typical flat-plate solar collector are shown in **Figure 2.1** below (Euro Journals, 2010) ^[8].

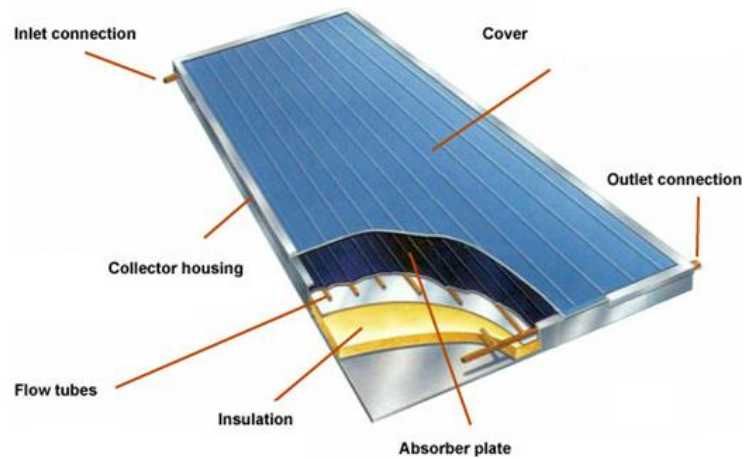


Figure 2.1 Pictorial view of a flat plate collector

The basic components that made up a flat plate solar collector are ^[2]:

- i. A flat blackened **absorber plate** made of any material; normally the one with high absorptivity and thermal conductivity, adequate tensile and compressive strength, and good corrosion resistance will rapidly absorbs heat from short wave solar radiation and quickly transfer that heat to the working fluid in the tubes to be carried away for storage or use.
- ii. **Transparent glazing cover** can either be single or multi layer sheets of glass through which the solar energy is transmitted are extremely important in the functioning of a collector. The functions of cover plate are to transmit maximum solar energy to the absorber plate, minimize upward heat loss from the absorber plate through convection and shield the absorber plate from direct exposure to weathering.
- iii. **Thermal insulation** provided at the back and sides of the absorber plate to minimize the heat losses minimizes from the solar collector.
- iv. **Flow tubes** or fins for conducting or directing the heat transfer fluid from the inlet header to the outlet. The liquid tubes can be welded to the absorbing plate, or they can be an integral part of the plate. The liquid tubes are connected at both ends by large diameter header tubes.
- v. **Collector housing**; a weather-tight container to enclose the above components and keeps them free from dust, moisture, etc.

2.1 Natural Convection inside Enclosure

Natural convection heat transfer inside a solar collector as in **Figure 2.2** is due to buoyancy forces and temperature changes in the heat transfer fluid between cover and absorber plate and is accomplished by displacement of the fluid. Y. Varol and H.F. Oztop^[9] stated that number of studies shown that the aspect ratio is the most important parameter affecting the heat and fluid flow. Higher heat transfer rate is obtained at lower aspect ratio but for a certain limit value for Grashof Number.

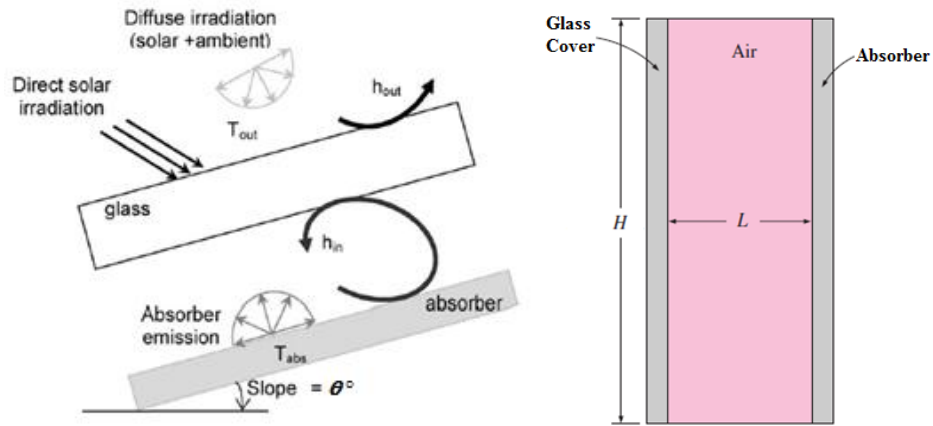


Figure 2.2 Analysis model of solar collector subjected to solar and thermal irradianations

$$Aspect\ ratio = \frac{H}{L} \quad (2.1)$$

According to Incropera and DeWitt^[10], the larger the temperature difference between the fluids to a hot or cold surface, the larger the buoyancy force and the stronger the natural convection currents. As a result, the higher heat transfer rate obtained.

For case hotter plate at the bottom, heavier fluid will be on top of the lighter fluid, and there will be a tendency for the lighter fluid to topple the heavier fluid and rises to the top. The heat transfer rate inside enclosure is defined as below:^[10]

The rate of heat transfer inside air heating solar collector:

$$Q = hA_s(T_{plate} - T_f) = \dot{m}C_p(T_{air,out} - T_{air,in}) \quad (2.2)$$

Convective Heat Transfer Coefficient, h:

$$h = \frac{Nuk}{L_c} \quad (2.3)$$

Where T_{plate} is the temperature of absorber plate ($^{\circ}\text{C}$); \bar{T}_f is the film temperature; \dot{m} is the mass flow of the air inside the channel (kg/s) which calculated from the products of air density(ρ), velocity of air (V) and area of the flow (A_s); C_p is the specific heat capacity of air (J/kg.K); $T_{air,out}$ and $T_{air,in}$ is the temperature of air at the outlet channel and inlet channel respectively ($^{\circ}\text{C}$); h is convective heat transfer coefficient ($\text{W}/\text{m}^2\text{K}$); Nu is the Nusselt number; k is the air thermal conductivity (W/mK) and L_c is the characteristic length of the channel (m).

Hydraulic Diameter (D_h)

According to Turns (2006) ^[11], for duct with circular cross section, the duct diameter D is employed as the characteristic length in correlation for heat transfer. However for a non circular duct such as rectangular passage, hydraulic diameter is employed as the characteristic length. Hydraulic diameter, D_h is defined as:

$$D_h = \frac{4 \times \text{flow cross sectional area}}{\text{wetted parameter}} \quad (2.4)$$

For a rectangular duct, if completely filled with fluid:

$$D_h = \frac{4LW}{2(L+W)} = \frac{2LW}{L+W} \quad (2.5)$$

Hence, the hydraulic diameter must be used as the characteristic length in every correlation governing for heat transfer in rectangular channel.

Prandtl Number (Pr)

The thickness of thermal boundary layer increases in the flow direction of liquid. The development of velocity boundary layer relative to thermal boundary layer will have strong effect on convection heat transfer. The relative thickness of the velocity and thermal boundary layers are described by the dimensionless parameter called as Prandtl number and is defined as in Eq. (2.6): ^[10]

$$Pr = \frac{\text{Kinematic Viscosity}}{\text{Thermal Diffusivity}} = \frac{\nu}{\alpha} = \frac{\mu C_p}{k} \quad (2.6)$$

The typical ranges of Prandtl number are shown in the **Table 2.1** below:

Table 2.1 Range of Prandtl number

Medium	Prandtl Number (Pr)
Liquid metals	0.004 – 0.030
Gases	0.7 – 1.0
Water	1.7 – 13.7
Oil	50 – 100,000

Thus, for air the Prandtl Number is assumed to be independent of temperature and is normally taken equal to **Pr = 0.7**.

Grashof Number, Gr

Grashof Number (Gr) is dimensionless which measure the relative magnitudes of the buoyancy forces and the opposing friction force acting on the fluid ^[10].

Gr, the ratio between the buoyancy force and viscous force inside enclosure is expressed as:

$$Gr = \frac{g\beta(T_{plate} - \bar{T}_f)D_h^3}{\nu^2} \quad (2.7)$$

All the fluid properties are evaluated at the **film temperature**, T_f as shown below.

$$T_f = \frac{T_{air, out} + T_{air, in}}{2} \quad (K) \quad (2.8)$$

Where

g = Gravitational acceleration, 9.8 m/s²

β = Coefficient of volume expansion, $\beta = \frac{1}{T_f}$

T_{plate} = Temperature of hot surface (absorber), °C

\bar{T}_f = Film temperature, °C

D_h = Hydraulic Diameter, m

ν = Kinematic viscosity, m²/s

In some cases, Grashof Number provides the main criterion in determining whether the fluid flow is laminar or turbulent. The critical Grashof number is **$Gr_{cr} = 10^9$** .

Rayleigh Number (Ra)

Rayleigh Number is the product of the Grashof number (**Gr**) in Eq. (2.7) and Prandtl number (**Pr**) in Eq. (2.6). For an inside enclosure, Rayleigh number (Ra) which is used in the heat transfer correlation is determined from^[10]:

$$Ra = Gr \cdot Pr = \frac{g\beta(T_{plate} - \bar{T}_f)D_h^3 Pr}{\nu^2} \quad (2.9)$$

Reynolds Number (Re)

Reynolds Number (*Re*) gives relation between inertial force and viscous force of fluid flow. They are used to characterize different flow regimes, such as laminar or turbulent flow: laminar flow occurs at low Reynolds numbers, where viscous forces are dominant, and is characterized by smooth, constant fluid motion; turbulent flow occurs at high Reynolds numbers^[10].

$$Re = \frac{\rho V L_c}{\mu} = \frac{V L_c}{\nu} = \frac{V D_h}{\nu} \quad (2.10)$$

Where

V = free stream velocity (m/s)

μ = dynamic viscosity of air ($kg/(m \cdot s)$)

ρ = density of air (kg/m^3)

D_h = hydraulic diameter

For **fluid flow over the flat surface**, the limit of laminar and turbulent flows is given as:

$$Re = 5 \times 10^5$$

According to Turns (2006)^[11], for **fluid flow through a pipe or duct**, the limit of laminar, transition and turbulent flows is determined from Reynolds number below.

$$\begin{aligned} \textit{Laminar} & : Re < 2300 \\ \textit{Turbulent} & : Re > 2300 \end{aligned}$$

Nusselt Number (Nu)

Nusselt number is selected based on the respective aspect ratios and Rayleigh number (Ra) in Eq. (2.9). It is an important parameter in determining the rate of heat transfer as well as the heat transfer coefficient. The correlation for Nusselt number varies for different convective heat transfer applications. The correlation of Nusselt number based on various cases is shown below:

i. Correlation for **horizontal rectangular enclosures**

Figure 2.3 below shows the horizontal rectangular enclosure at which $\theta = 0^\circ$, its Nusselt number can be calculated using Eq. (2.11).

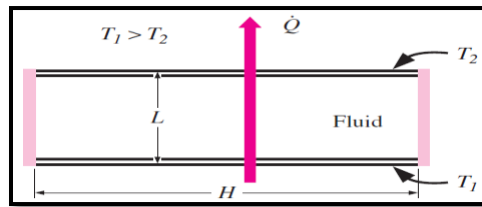


Figure 2.3 Horizontal rectangular enclosure

$$Nu = 1 + 1.44 \left(1 - \frac{1708}{Ra} \right) + \left[\left(\frac{Ra}{5830} \right)^{1/3} - 1 \right] \quad (2.11)$$

This correlation of Nusselt number is only valid for $Ra < 10^8$.

ii. Correlation for **inclined rectangular enclosures**

Table 2.2 Critical angle for inclined rectangular cavities

(H / L)	1	3	6	12	> 12
τ^*	25°	53°	60°	67°	70°

Typically, transition between two types of flow motion occurs at critical tilt angle, τ^* with a corresponding change in Nu. For large aspect ratio ($H/L \geq 12$) and tilt angles less than critical values, τ^* given in **Table 2.2**, the following correlation due to Hollands et al. ^[12] is in excellent agreement with the available data:

For $Pr \approx 0.7$; $Ra < 10^5$; aspect ratio: $H/L \geq 12$ and inclination angle at $0^\circ < \theta \leq 70^\circ$ for system as in **Figure 2.4**, its Nusselt no. can be determined from Eq. (2.12) below:

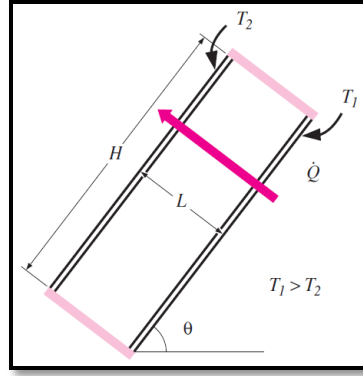


Figure 2.4 Inclined rectangular enclosure

$$Nu = 1 + 1.44 \left[1 - \frac{1708}{Ra \cos \theta} \right] \cdot \left[1 - \frac{1708 (\sin 1.8 \theta)^{1.6}}{Ra \cos \theta} \right] + \left[\left(\frac{Ra \cos \theta}{5830} \right)^{\frac{1}{3}} - 1 \right] \quad (2.12)$$

Beyond the critical tilt angle, the following correlation due to Ayyaswamy and Colton^[13] has been recommended for all aspect ratios (H/L):

$$Nu = Nu(\tau = 90^\circ) (\sin \tau^*)^{1.4} \quad (\tau^* \leq \theta < 90^\circ) \quad (2.13)$$

iii. Correlation for **vertical rectangular enclosures**

In case of vertical rectangular enclosure where $\theta = 90^\circ$ as in **Figure 2.5**, the Nusselt number is dependent on the aspect ratio H/L of the enclosure.

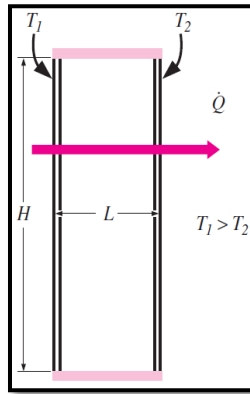


Figure 2.5 Vertical rectangular enclosure

For small aspect ratios, Catton (1978)^[14] has suggested the following correlation:

For $1 < H/L < 2$

$$Nu = 0.18 \left(\frac{Pr}{0.2 + Pr} Ra \right)^{0.29} \quad (2.14)$$

For $2 < H/L < 10$

$$Nu = 0.22 \left(\frac{Pr}{0.2 + Pr} Ra \right)^{0.28} \left(\frac{H}{L} \right)^{-\frac{1}{4}} \quad (2.15)$$

While for larger aspect ratios, the following correlation is proposed by MacGregor and Emery (1969):^[15]

For $10 < H/L < 40$

$$Nu = 0.42 Ra^{\frac{1}{4}} Pr^{0.012} \left(\frac{H}{L} \right)^{-0.3} \quad (2.16)$$

A. Effect of Inclination Angle on Heat Transfer

Various studies have been conducted all over the world to investigate the effect of inclination angle on heat transfer rate or efficiency of a solar collector. M.Premalatha, S.Shanmuga, and A.Saravanakumar^[16] conducted an experimental investigation on inclination angle on heat transfer characteristics on wickless solar heat pipe. They observed that the heat transfer efficiency increases with inclination angle and reaches a maximum at about 45° and the steeper the tube, the larger the heat flow rate. The effect of inclination angle on the efficiency indicates that the maximum efficiency is observed at angles of $40^\circ - 45^\circ$.

Matuszewski and Sawicka (2010)^[17] concluded their thesis on optimization of solar air collector by stating that for a collector operating through the whole year the best effect would be obtained when the panel was set with angle 37.5° as it exposed to higher amount of solar radiation. From experimental investigation on convection heat transfer in flat plate solar collector conducted by Toh Seng Peow (2011)^[18], it is observed that insolation intensity is significantly affected by the tilt angle. The system is gaining higher incident solar radiation at lower inclination angle, thus providing higher value of insolation.

Sertkaya, Bilir, and Kargici^[19] studies on convection heat transfer on pinned fin surface discovered that the enhancement of heat transfer on the pinned fin surface is decreasing with increasing orientation angle from the vertical axis. For inclination

angle which allowed the pinned fin upfacing the solar radiation, the heat transfer is higher than when the pinned surface downfacing the sunlight.

B. Effect of Different Channel Length

Bashria and Mariah ^[20] investigation on the effect of mass flow, channel depth and collector length on the thermal performance and pressure drop through flat plate solar collectors found that the channel length also has significant effect on the thermal efficiency. The system efficiency is more increased for the shorter channel length of 1.5 m; but the outlet temperature is higher for long channel length 2.4m than for the shorter 1.5 m channel length.

C. Effect of Pinned Plate versus Flat Plate

Based on the experimental investigation carried by Sertkaya, Bilir, and Kargici ^[19] on the natural convection heat transfer in air from a pin-finned surface by considering the effect of radiation heat transfer, they observed that the heat transfer by free convection on the pin finned plate increased significantly compared to the unpinned surface (flat plate).

D. Effect of Staggered Pinned Plates on Turbulence and Heat Transfer

Turbulent boundary layers over rough surfaces have considerable engineering interest due to the increased transport of heat and mass which is usually associated with an increase in momentum transport. According to Krogstad and Antonia (1999) ^[21], the effects of surface roughness on the mean velocity and temperature profiles are well known although there is still some difficulty in identifying a length scale that characterizes particular roughness geometry. On the other hand, considerable uncertainty exists with respect to the effect a rough surface has on turbulent quantities. Their experimental investigation on surface roughness effects in turbulent boundary layers proven that the surface geometry significantly affects the turbulent characteristics of the flow.

Besides, Karthikeyan et al. ^[22] have concluded his experimental analysis on fin-pin heat exchanger to study the flow and thermal characteristics by stating that the staggered pin-fin array significantly enhanced heat transfer as a result turbulence

but in return experienced higher pressure drop in the wind tunnel. Boelter et al. (1950) ^[23] also have conducted an experimental determination on the thermal and hydrodynamical behaviour of air flowing on the finned plate. The results indicate that the effect of added turbulence along the plate due to the presence of the pin fin shows an increment in heat transfer rate of as high as 75 percent because the pin fins added the heat transfer area. The velocity distribution also changes due to the presence of these extended surfaces. **Figure 2.6** illustrates the pin array arrangement.

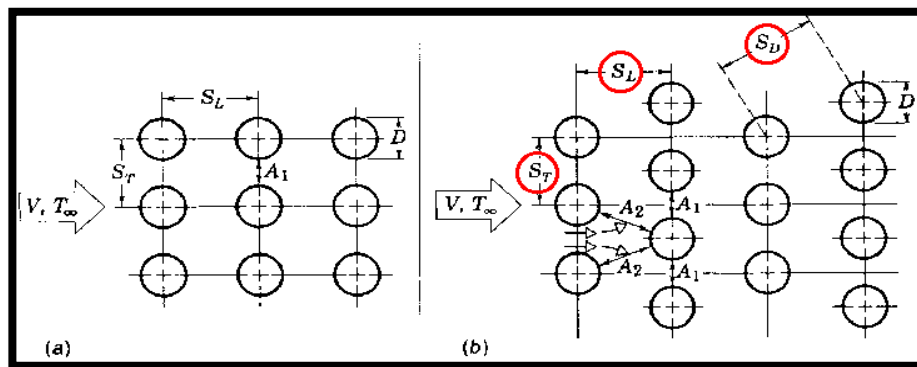


Figure 2.6: a) In-Line or Parallel arrangement b) Staggered arrangement

E. Effect of Pin Height (H) on Heat Transfer

Brigham and VanFossen (1984) ^[24] investigated the effect of pin height on array-averaged heat transfer. The results showed that for height to diameter (H/D) ratio as shown in **Figure 2.7** less than three; there is no effect on array-averaged heat transfer whereas for H/D greater than three the heat transfer significantly increases with increasing H/D. This condition can be explained by Armstrong and Winstanley (1988) ^[25] who stated that pin heat transfer is dominated by the end wall interactions. As for short pins, the endwalls make up a significant portion of the heat transfer surface. But as the pins lengthen, a greater portion of the heat transfer surface area is now comprised by the pin; thus the endwall - pin interactions no longer dominate the flow near the centre of the channel.

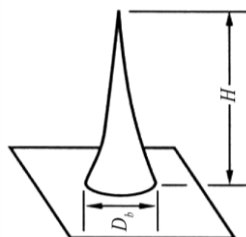


Figure 2.7 Pin fin geometry

CHAPTER 3

METHODOLOGY

3.1 Research Methodology

Primarily, self-reference towards existing network documents, websites, research papers, journals, books, encyclopaedias and etc. have become the main research sources throughout this project. To ensure this project is on the right track, it need to closely follows the “Analytical and Experimental Investigation of Convection Heat Transfer in Flat Plate Solar Collector” project by Toh Seng Peow [14]. For analytical data collection, series of experiments were conducted on the staggered pinned plate solar collector test rigs; ran at three different variables which are:

- i. Different inclination angles of 10° , 30° , 50° , 70° and 90° with respect to the horizontal base
- ii. Different pins height on the absorber plates – 2mm, 3mm and 4mm
- iii. Type of absorber plate (flat and staggered pinned plate)

Pins with staggered orientation at specified spacing or gaps introduced throughout the surface of Aluminium absorber plates of the solar collector according to the dimension specification shown on the illustration in **Figure 3.1** below.

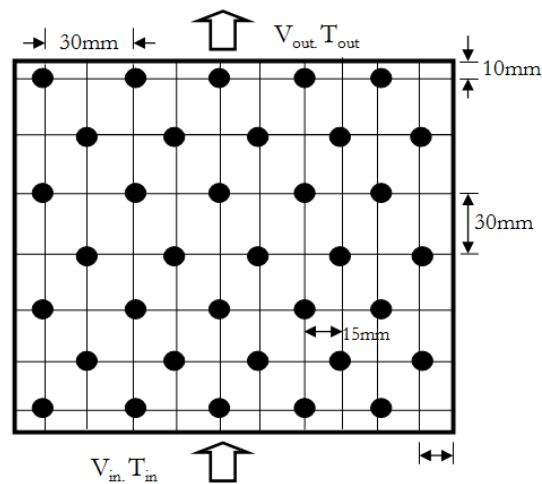


Figure 3.1 Geometry of staggered pinned plate

The readings are measured at interval of 2 hours from 8 am to 6pm. Three staggered pinned plates and one flat plate absorber are tested using 4 solar collector test rigs simultaneously; 4 days for each inclination angle which resulted in total of 20 days of experimental data collection. The parameters that are recorded from the experiment are listed as below and shown in **Figure 3.2**:

- i. Temperature of outer (G_1) and inner (G_2) glazing cover
- ii. Temperature of staggered absorber plate (A) and the flat absorber plate
- iii. Ambient temperature (T_{amb}) and outlet air (T_{out}) temperature of the solar collector
- iv. Solar insolation (S)
- v. Ambient wind speed, $V_{ambient}$
- vi. The air velocity at the channel outlet, V_{out}

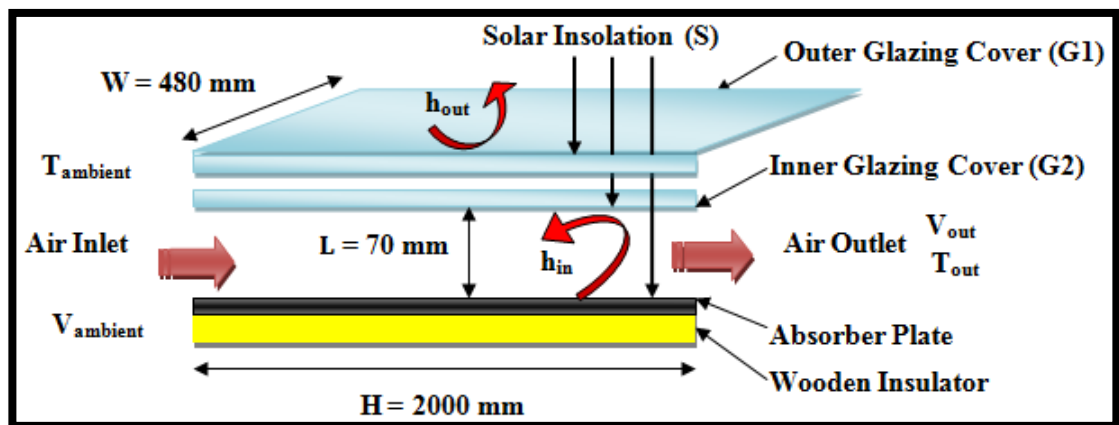


Figure 3.2 Physical model of double glazing solar collector

3.2 Project Activities Flow Chart

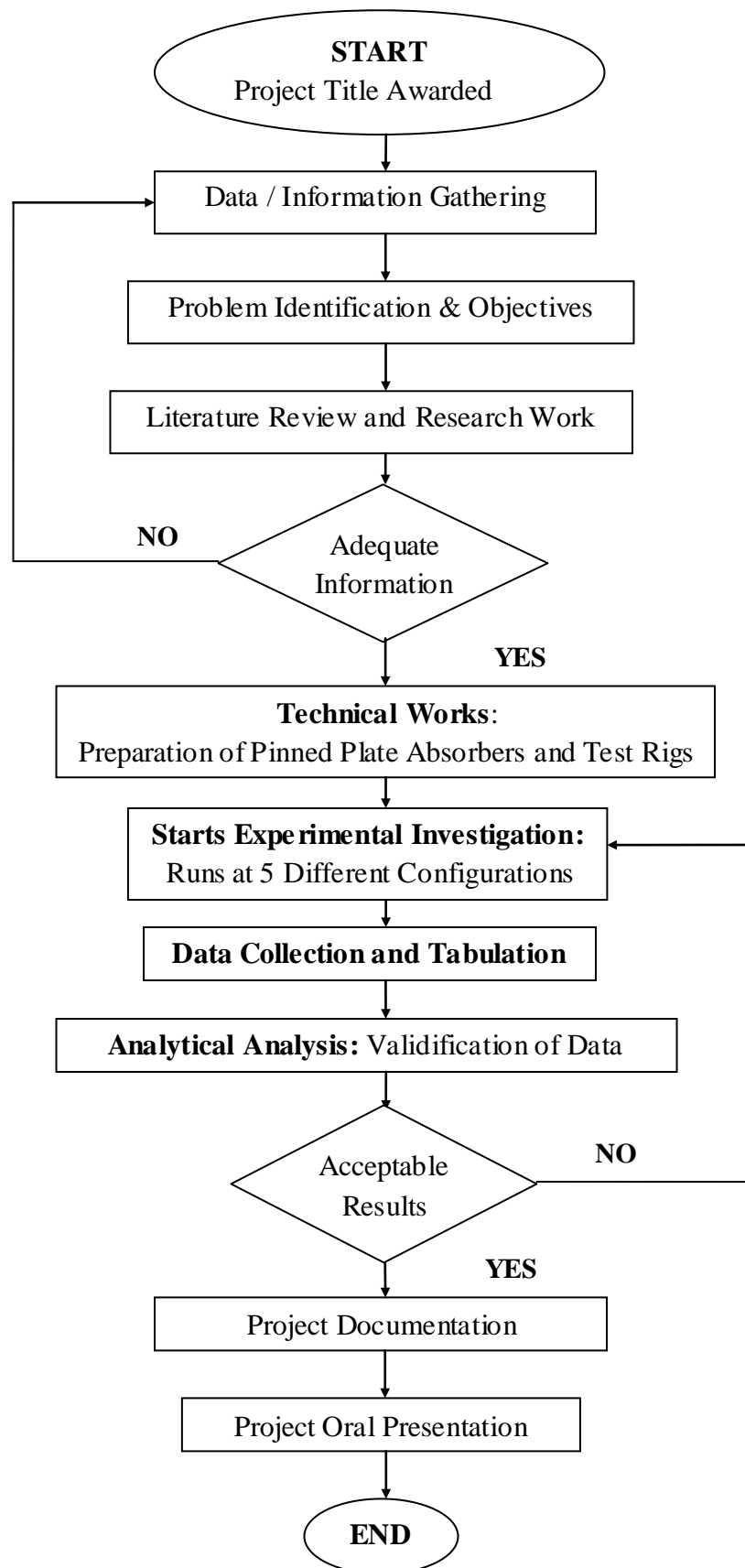


Figure 3.3 Project activities flow chart

3.3 Analytical Analysis

3.3.1 Methodology for Determining Rate of Heat Transfer (\dot{Q})

- i. Determine the fluid properties based on film temperature using Eq. (2.8) such as Prandtl number, kinematic viscosity and thermal conductivity.
- ii. Identify the characteristic length, L_c of the system which is the hydraulic diameter, D_h using Eq. (2.5) since it is noncircular duct.
- iii. Calculate the heat transfer rate or heat loss using Eq. (2.2)
- iv. Calculate convective heat transfer coefficient using Eq. (2.3) thus can determine the respective Nusselt number.
- v. Calculate the Rayleigh number by Eq. (2.9) as product of Grashof, Eq. (2.7) and Prandtl number, Eq. (2.6).
- vi. Determine air flow behaviour or type by Reynolds number through Eq. (2.10)

3.3.2 Validation of Nusselt Number and Natural Convection

According to Holman (2010) [26], for free or natural convection to occur, the following criterion must be satisfied.

$$\frac{Gr}{Re^2} > 10 \quad (3.1)$$

Figure 3.4 and Figure 3.5 presents the regime of free, forced and mixed convection for flow through vertical and horizontal tube respectively.

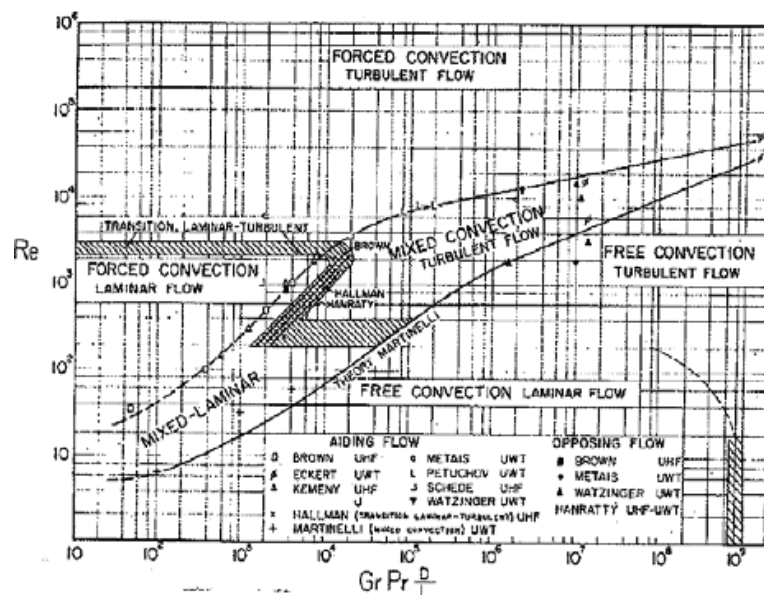


Figure 3.4 Regime of free, forced and mixed convection for flow through vertical tubes according to Metais and Eckert [27]

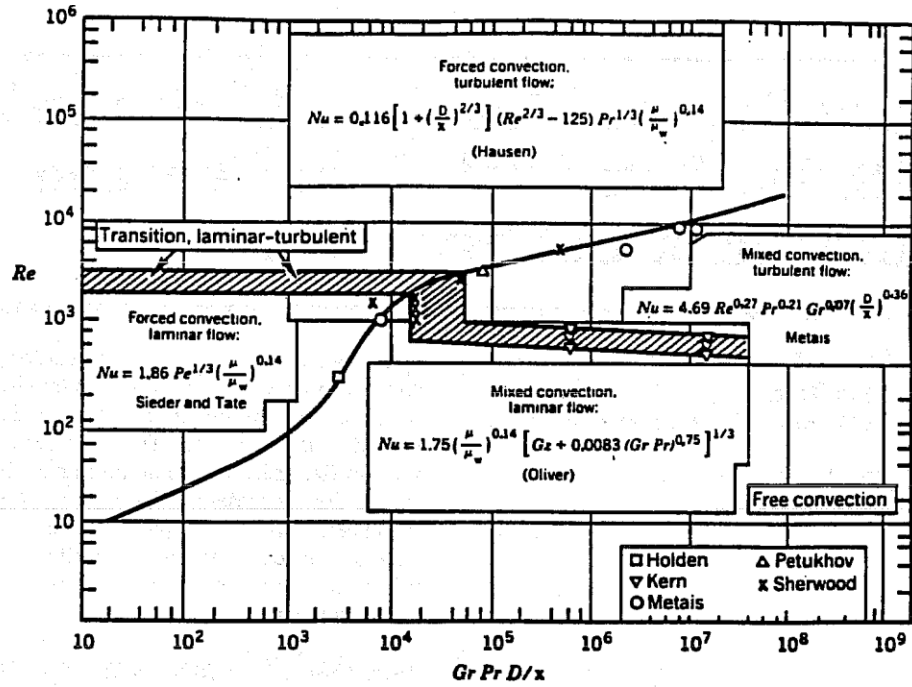


Figure 3.5 Regime of free, forced and mixed convection for flow through horizontal tubes according to Metais and Eckert [27]

In Figure 3.5, the Graetz number is defined as:

$$Gz = RePr \left(\frac{D_h}{L} \right) \quad (3.2)$$

Applicable ranges for Figure 3.4 and 3.5 [26] is for

$$10^{-2} < Pr \left(\frac{D_h}{L} \right) < 1 \quad (3.3)$$

Nusselt number calculated using Eqs. (2.11-2.15) is validated by comparing with Nusselt no. from Eqs. (3.4-3.6) shown below. Brown and Gavin [28] have developed a better correlation for the mixed convection, laminar flow regime of Figure 3.5

$$Nu = 1.75 \left(\frac{\mu_b}{\mu_w} \right)^{0.14} \left(Gz + 0.012 (Gz Gr^{1/3})^{4/3} \right)^{1/3} \quad (3.4)$$

Mixed convection Turbulent Flow Regime of Figure 3.5

$$Nu = 4.69 Re^{0.27} Pr^{0.21} Gr^{0.07} \left(\frac{D_h}{L} \right)^{0.36} \quad (3.5)$$

Nusselt number as proposed by Lloyd and Moran (1974) [29] for natural convection.

$$Nu = 0.54 Ra \frac{1}{4} \quad (3.6)$$

3.4 Key Milestones

Table 3.1 below shows the activities in Key Milestone with the detailed timeline.

Table 3.1 Timeline for each key milestone

Project Activities	Week	Date start	Date End
Final Year Project I			
Extended Proposal Submission	6	25 June 2012	1 July 2012
Proposal Defence	8-10	9 July 2012	29 July 2012
Interim Report Draft Submission	12	6 Aug 2012	12 Aug 2012
Interim Report Submission	13	13 Aug 2012	16 Aug 2012
Final Year Project II			
Progress Report Submission	8	5 Nov 2012	11 Nov 2012
Pre- EDX	11	26 Nov 2012	2 Dec 2012
Draft Report Submission	12	3 Dec 2012	9 Dec 2012
Dissertation Submission	13	10 Dec 2012	16 Dec 2012
Technical Paper Submission	13	10 Dec 2012	16 Dec 2012
Oral Presentation	14	17 Dec 2012	23 Dec 2012
Dissertation Submission (Hard Bound)	15	24 Dec 2012	30 Dec 2012

3.5 Project Gantt Chart

Final Year Project I

Table 3.2 Final Year Project I Project Gantt chart

No	Project Activities / Week	1	2	3	4	5	6	7	8	9	10	11	12	13	14	
1	Project Title Selection							Mid Semester Break								
2	Preliminary Research Work															
3	Literature Review															
4	Build pinned absorber plate															
4	Submission of Extended Proposal															
5	Proposal Defence															
7	Submission of Interim Draft Report															
8	Submission of Interim Report															

Final Year Project II

Table 3.3 Final Year Project II Project Gantt chart

No	Project Activities / Week	1	2	3	4	5	6	7	8	9	10	11	12	13	14	15	
1	Start experiments	█	█	█	█	█	█	Mid Semester Break	█	█	█						
2	Analytical analysis	█	█	█	█	█	█		█	█	█						
3	Result Analysis					█	█		█	█	█	█	█				
4	Report writing		█	█	█	█	█		█	█	█	█	█	█	█		
5	Progress Report Submission									█							
6	Pre-EDX preparation									█	█	█					
7	Pre-EDX												█				
8	Draft Report Submission													█			
9	Dissertation Submission														█		
10	Technical Paper Submission															█	
11	Oral Presentation																█
13	Project Dissertation Submission (Hard Bound)																█

 **Key Milestones**

 **Process**

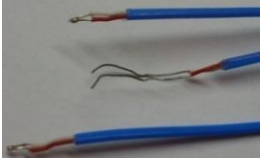
3.6 Tools and Software

One of the important aspects in completing a project is the correct selection and usage of tools and software. Suitable tools and software are crucial so that it will not cause any trouble that tends to obstruct the flow of the project completion later. In order to complete this project, the software and tools that were used are shown in **Table 3.4** and **Table 3.5** respectively.

Table 3.4 Software and their purposes

No	Software	Purpose
1	Microsoft Excel 2007	For result tabulation and graph plotting
2	Microsoft Word 2007	For documentation purpose
3	CATIA V5	For design modelling purposes

Table 3.5 Equipments and their purposes

No	Equipment / Tools	Purpose
1	Test Rigs (Figure 3.6 to 3.10)	To serve as solar collectors
2	Channels data logger 	To record temperature of the outlet air, the surface temperature of absorber plates as well as the glazing covers.
3	Thermocouple wires 	Attached to the surfaces of double glazing covers and absorber plates and connected to data logger to measure their surface temperatures.
4	Data Logger Thermometer 	To measure inner and outer air temperature of the solar collectors; as backup if the temperature recorded by data logger shows some error.
5	Solarimeter 	To measure angular solar insolation at the solar site for each interval.
7	Pin punchers 	To create pins on the solar collector absorber plates at different pins height of 2mm, 3mm and 4mm.
8	Anemometer 	To measure the ambient wind speed and temperature for each interval.
9	Flow Sensor 	To measure the velocity of air at the channel outlet in term of voltage.

3.7 Experimental Setup

Figure 3.6, 3.7 3.8, 3.9 and 3.10 below shows the solar collector test rigs of 2m passage length used for this experimental work at five different configurations which is 10° , 30° , 50° , 70° and 90° inclination angle respectively.



Figure 3.6 Test rigs at 10° inclination angle



Figure 3.7 Test rigs at 30° inclination angle



Figure 3.8 Test rigs at 50° inclination angle

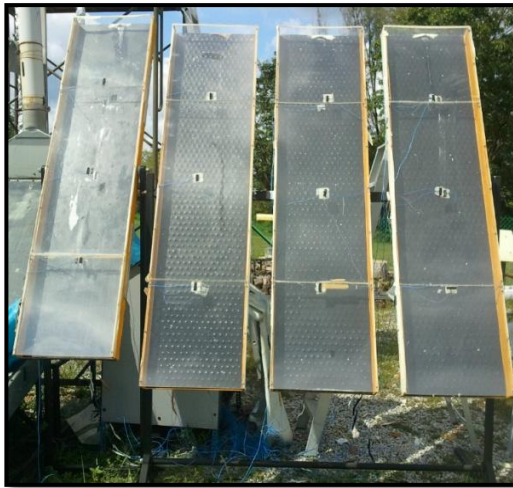


Figure 3.9 Test rigs at 70° tilt angle



Figure 3.10 Test rigs at 90° tilt angle

For this project purpose, sets of test rigs are fabricated using the same model and specifications as the Toh Seng Peow's ^[18] solar collector test rig. In order to reduce the cost of production, at the same time increase the ease of transportation, fabrication and configuration, the test rigs are designed to be attachable and detachable to satisfy the different length configuration. The supporters are used to support the rectangular passage with adjustable lock to ensure the rectangular passage could be oriented or tilted to any desired angle (in this case 10°, 30°, 50°, 70° and 90° with respect to the horizontal base).

The supporters are directly attached to the 1m rectangular passage; meanwhile the 0.5m section(s) can be attached to the 1m rectangular passage by clipper or hinge to achieve 1.5m and 2m respectively. Accordingly, the insulators and double glazing are also extended to the required length throughout the experiment. However, unlike insulators the absorber plates are not extended. Different absorber plates will be manually fixed to the insulator based on the desired configuration of 1m, 1.5m and 2m respectively. But for this project, the required passage length is only 2m. The solar collector test rig with attachable and detachable 0.5m rectangular passage is illustrated in **Figure 3.11** as shown below:

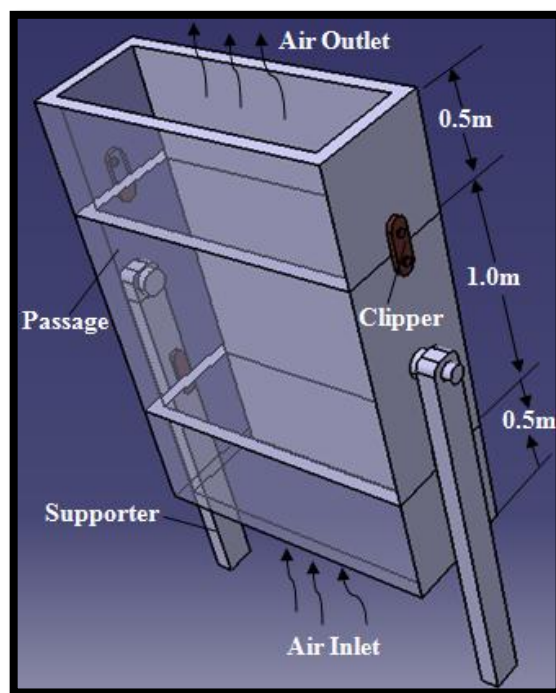


Figure 3.11 Isometric view of the solar collector test rig

The thermocouple wires which are connected to data logger are being placed along the length of the surfaces of the inner and outer glazing covers as well as the absorber plates to measure their respective mean wall temperatures. The thermocouple wires are also placed at the outlet of each collector to measure the outlet air temperature. The wooden containers which provided insulation to the system were painted with flexible waterproof sealer to reduce the effect of water (rain) on the plywood while absorber plates were painted black to increase their absorptivity. In addition, the tiny gaps between the glazing covers were sealed with silicon tape to minimize the heat losses during the convection heat transfer process.

CHAPTER 4

RESULTS AND DISCUSSION

As mentioned in the previous section, each of the configurations (tilt angle) is repeated for 4 days to improve the reliability of the result by taking the average reading. Despite that average readings have considered, it is necessary to clarify that the data collected are sometime inconsistent, due to the inevitable sudden change of weather. Throughout the experiments, the weather is changing too frequently; cloudy and raining which by observation; frequently occurs at 4pm onwards thus data such the ambient temperature and wind speed, solar intensity as well as the outlet air velocity cannot be measured at that particular time. The experiments are completed for 10°, 30°, 50°, 70° and 90° inclination angles only for 2m absorber plates. The results of the completed experiments are shown below and following graphs are plotted against time and inclination angles to observe the transient behaviour of the system. **Table 4.1** and **Figure 4.1** below show the intensity of solar insolation for all inclination angles at each interval.

Table 4.1 Solar insolation intensity at different inclination angle

Angle	10°	30°	50°	70°	90°
Time	Insolation (W/m ²)				
08:00	102.33	121.42	154.30	38.33	12.00
10:00	638.00	368.70	368.73	343.90	270.00
12:00	753.00	665.83	630.38	526.77	515.00
14:00	482.02	502.93	527.70	224.67	235.00
16:00	73.00	115.28	328.67	215.00	253.00
18:00	55.51	3.54	7.05	10.00	29.00

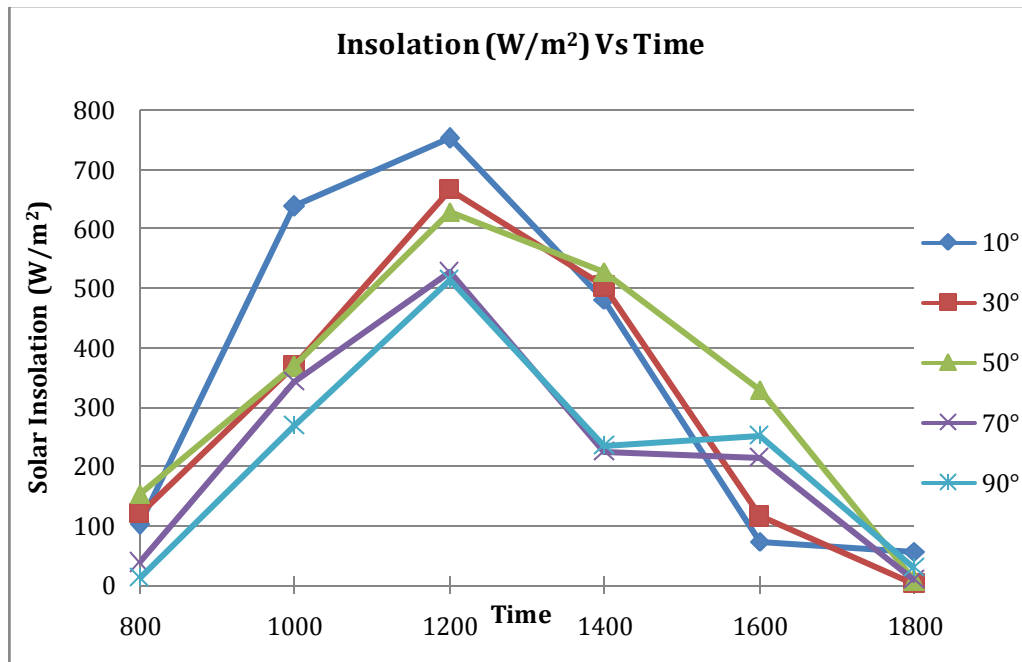


Figure 4.1 Insolation profile at different inclination angles

Since the experiment is conducted simultaneously using 4 test rigs, the solar insolation is considered similar for all the absorber plates having the same length at each configuration. Therefore, the solar insolation can only be compared due to effect the inclination angle rather than the type of absorber plates (staggered or flat plate). However, since for each angle the experimental works were conducted separately at different days, the solar insolation is dependant mostly on the weather for that particular day. Thus, it is not really practical to compare the effect of inclination angle on the intensity of solar radiation as the weather is not constant throughout the experimental days.

However, it is observed that the solar radiation intensity reaching its peak around 12 pm to 2pm and then gradually decreasing afterwards for all the inclination angles tested. The insolation at 10° inclination angle shows the highest intensity during peak times compared to other configurations since the system is exposed to higher incident of solar radiation at lower tilt angle. **Table 4.2** below show the measured air outlet temperature for pinned and flat absorber plates tested at 5 different configuration or inclination angles. In addition, the variation of air outlet temperature against the inclination angles for different absorber plates types are plotted and are displayed as **Figure 4.2, 4.3, 4.4, 4.5, 4.6** and **4.7** below.

Table 4.2 Air outlet temperature at different inclination angle

INCLINATION ANGLE		10°	30°	50°	70°	90°
TYPES	TIME	Air Outlet Temperature, T_{out} (°C)				
2MM PINNED PLATE ABSORBER	0800	26.63	27.63	28.92	28.46	28.52
	1000	40.47	43.08	44.57	40.84	40.77
	1200	52.20	46.58	51.93	49.08	43.43
	1400	28.67	44.35	46.33	42.43	41.65
	1600	29.43	29.04	37.36	45.80	52.42
	1800	25.53	25.73	28.20	33.15	42.08
3MM PINNED PLATE ABSORBER	0800	26.23	27.19	28.38	27.69	28.43
	1000	44.53	43.18	43.08	40.17	39.62
	1200	46.98	46.12	50.24	47.48	43.13
	1400	28.88	42.93	45.88	42.35	42.73
	1600	29.93	28.63	37.17	45.05	53.18
	1800	25.78	25.13	27.65	32.40	41.58
4MM PINNED PLATE ABSORBER	0800	26.20	27.73	28.60	28.20	29.79
	1000	40.55	43.11	43.64	39.42	40.12
	1200	50.87	45.24	50.11	46.80	42.42
	1400	28.10	43.18	45.11	40.99	41.18
	1600	28.38	28.43	36.46	44.59	51.23
	1800	25.78	25.53	28.13	33.15	41.32
FLAT PLATE	0800	26.02	26.34	26.92	26.84	27.15
	1000	40.08	39.39	40.95	36.66	37.88
	1200	43.35	40.92	45.99	43.50	42.34
	1400	27.15	39.56	42.93	40.62	41.71
	1600	27.95	27.70	35.23	43.58	51.89
	1800	25.65	25.08	27.11	32.52	40.96

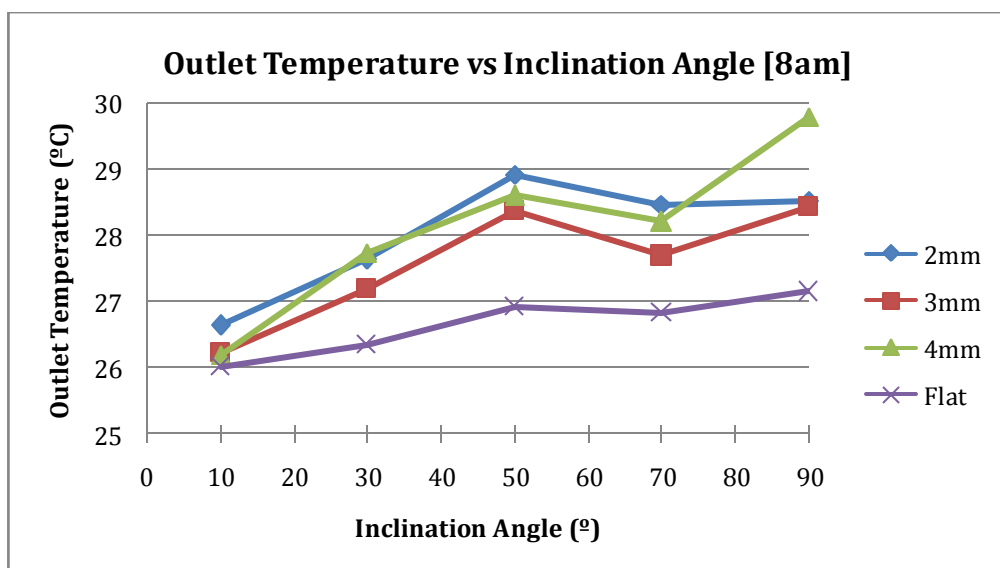


Figure 4.2 Outlet temperature profile for inclination angle at 08:00

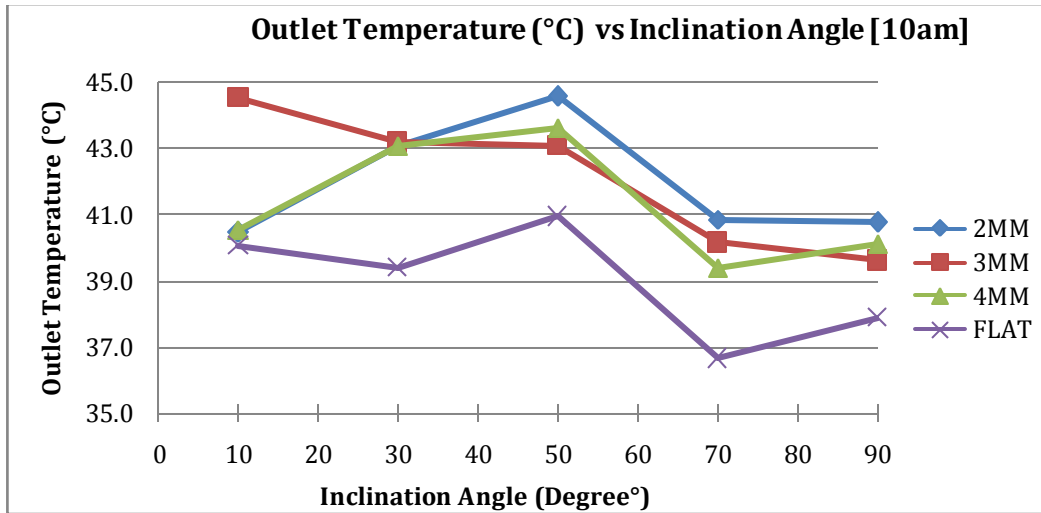


Figure 4.3 Outlet temperature profile for inclination angle at 10:00

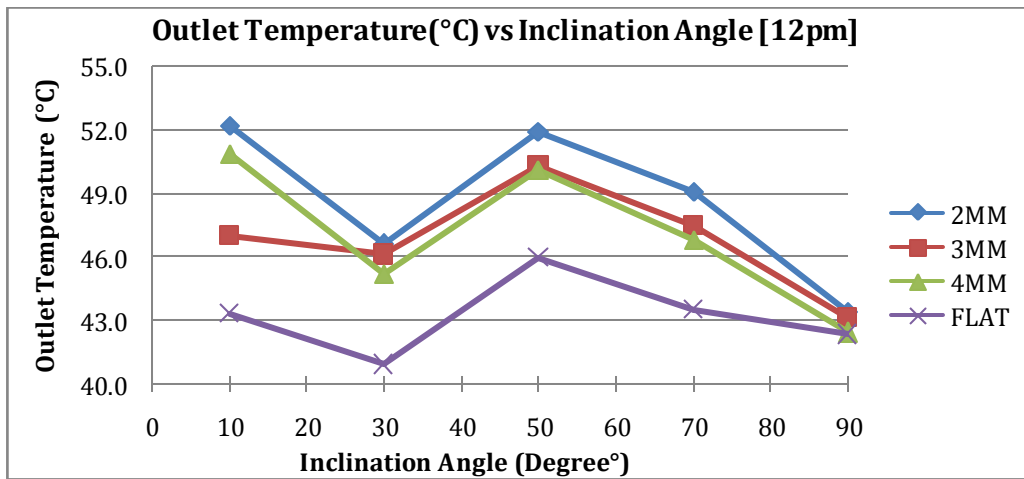


Figure 4.4 Outlet temperature profile for inclination angle at 12:00

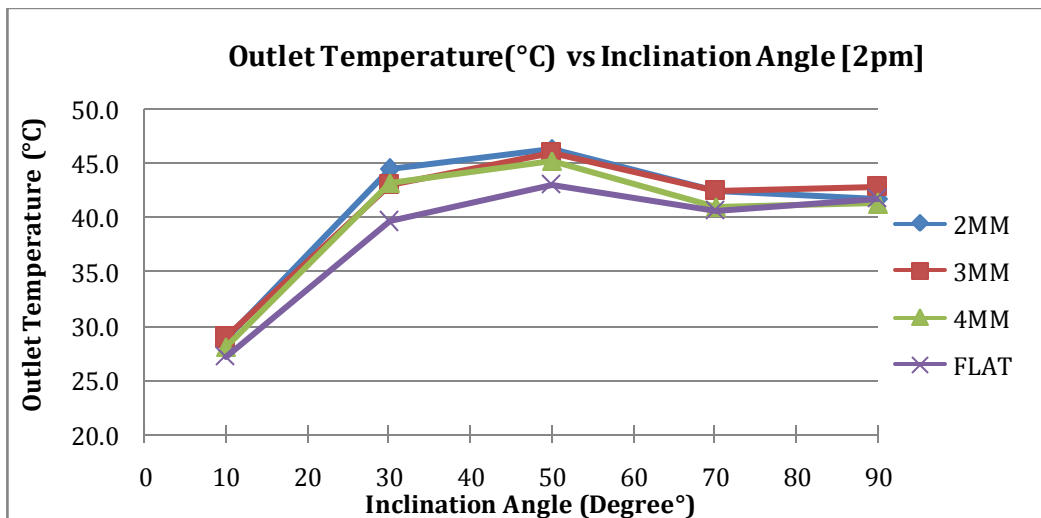


Figure 4.5 Outlet temperature profile for inclination angle at 14:00

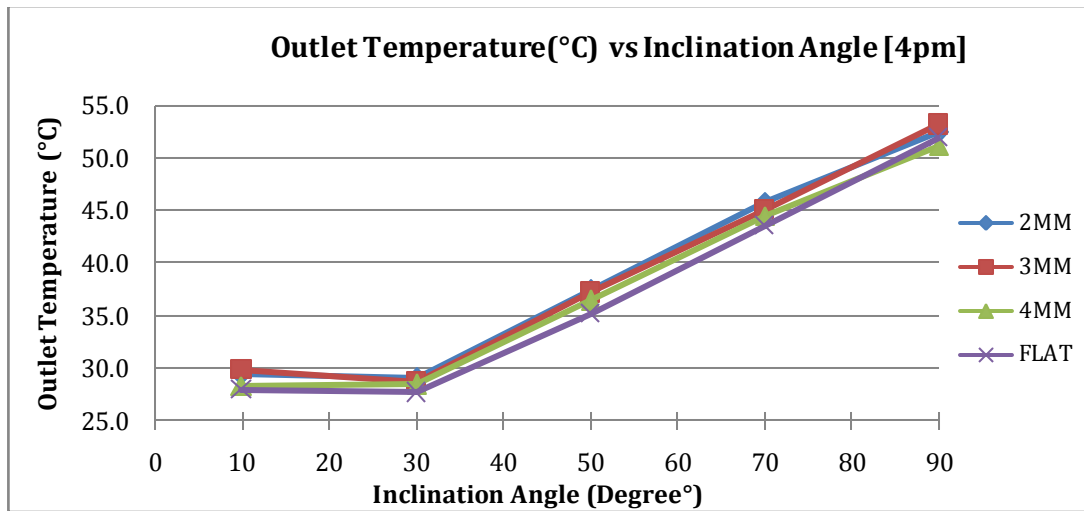


Figure 4.6 Outlet temperature profile for inclination angle at 16:00

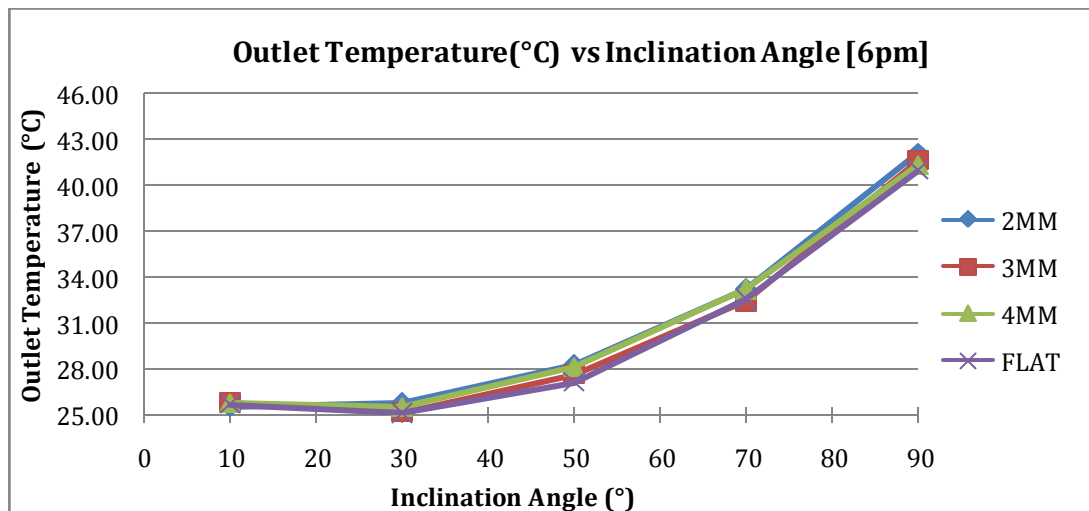


Figure 4.7 Outlet temperature profile for inclination angle at 18:00

Based on these figures, as overall it can be seen that for each time interval the system with 2mm pinned absorber plate is having the highest outlet temperature followed by system with 3mm and 4mm pinned absorber plate compared to a normal flat plate. The air outlet temperatures for staggered pinned absorber plates are always higher than the flat plate absorber for all provided the same ambient temperature for the systems. In this case, for pinned plate absorbers; the outlet temperature is higher for shorter pins height. The variation in outlet temperatures for all systems matched closely with the solar intensity profile where it gradually increasing from 8am, reaching its peak temperature around 12 pm to 2 pm and then gradually decreasing afterwards. Except at 4pm and 6pm due to frequently changed weather, the systems at 50° inclination angle configuration produce the highest air outlet temperature than

another configuration. It can be explained by considering the effect of wind which displacing the hot air out from the rectangular passage. For system at lower inclination angle where it absorbed more solar radiation, the effect of wind is higher as the position during this configuration almost parallel to direction of wind thus it can easily pass through the passage to displaced more hot air by cooler ambient air. Yet, for higher inclination angle system where the effect of wind can be reduced, these positions received less incident of solar radiation. Thus, the best position is in between horizontal and vertical axis which in this case is about 50° inclination angle.

In order to investigate the effect of **inclination angle** on heat transfer, the following graphs have been plotted as shown in **Figure 4.8** to **4.11**. The analyzed data for convective heat transfer coefficient has been tabulated as in **Table 4.3**.

Table 4.3 Convective heat transfer coefficient at different inclination angle and absorber types

INCLINATION ANGLE		10°	30°	50°	70°	90°
TYPES	TIME	Convective Heat transfer Coefficient, h (W/m ² K)				
2MM PINNED PLATE ABSORBER	0800	51.760	2.601	178.510	1.093	0.000
	1000	120.722	310.032	531.197	339.901	227.389
	1200	474.961	280.841	567.867	475.608	290.111
	1400	118.322	336.565	412.313	340.991	292.934
	1600	119.565	49.327	233.230	209.651	387.571
	1800	3.262	11.784	151.818	30.003	254.050
3MM PINNED PLATE ABSORBER	0800	18.083	0.416	124.015	0.000	0.000
	1000	208.586	237.559	409.454	351.998	265.250
	1200	229.770	286.468	454.966	384.584	206.480
	1400	253.651	254.972	383.045	343.876	387.977
	1600	155.227	25.456	229.236	170.426	468.815
	1800	51.338	2.314	131.512	5.204	352.710
4MM PINNED PLATE ABSORBER	0800	27.241	0.000	129.291	0.000	0.000
	1000	143.617	218.701	433.077	313.963	186.532
	1200	518.007	272.083	447.762	364.966	206.816
	1400	170.978	149.660	320.097	245.149	344.085
	1600	65.476	12.083	175.644	180.194	295.460
	1800	25.064	1.932	158.514	121.408	208.236
FLAT PLATE ABSORBER	0800	2.309	0.519	43.023	1.044	0.000
	1000	206.827	242.248	458.694	240.100	147.899
	1200	151.537	194.082	446.077	400.370	144.351
	1400	22.555	202.901	589.993	389.039	349.003
	1600	11.541	6.466	276.119	136.139	320.545
	1800	73.201	2.726	174.170	38.481	201.660

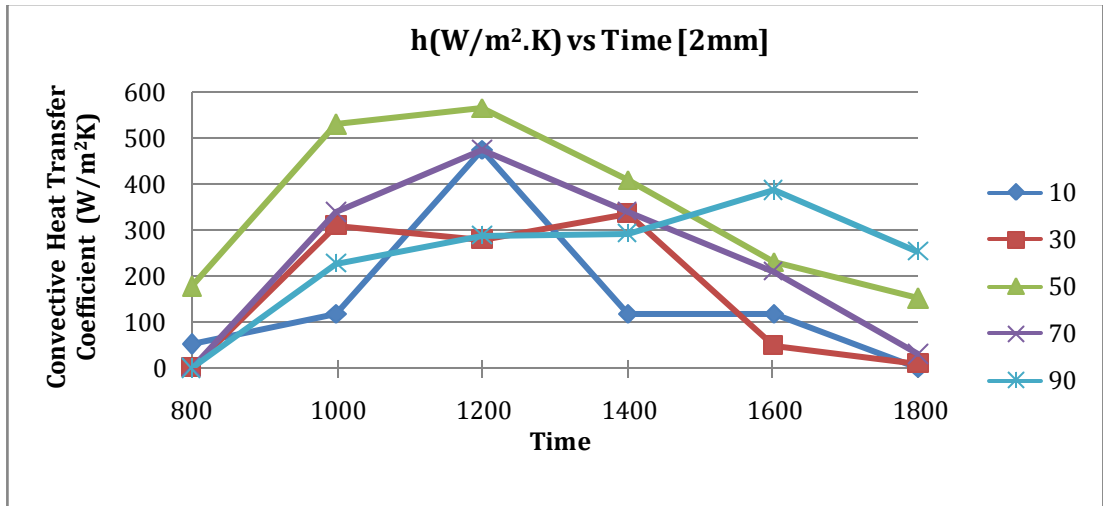


Figure 4.8 Convective heat transfer coefficient for 2mm pinned plate

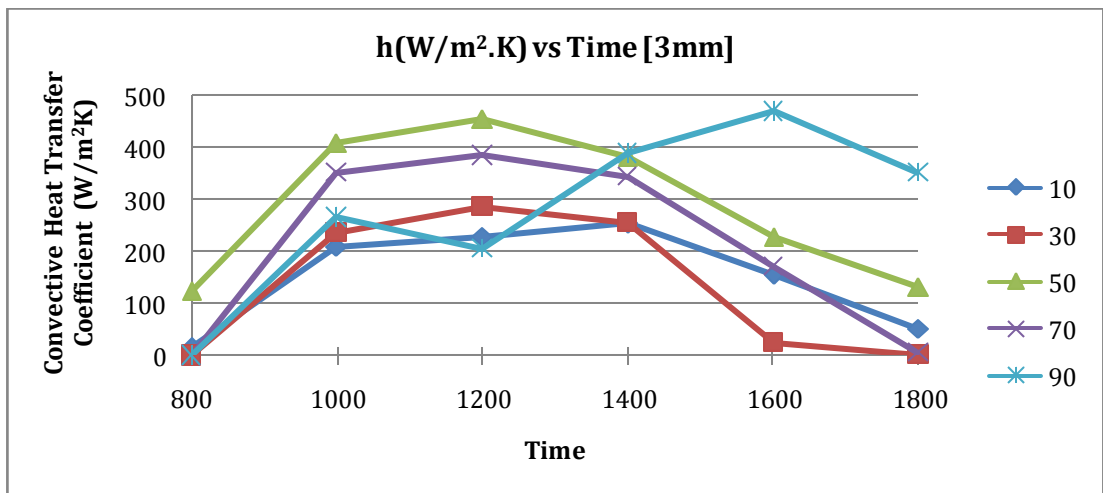


Figure 4.9 Convective heat transfer coefficient for 3mm pinned plate

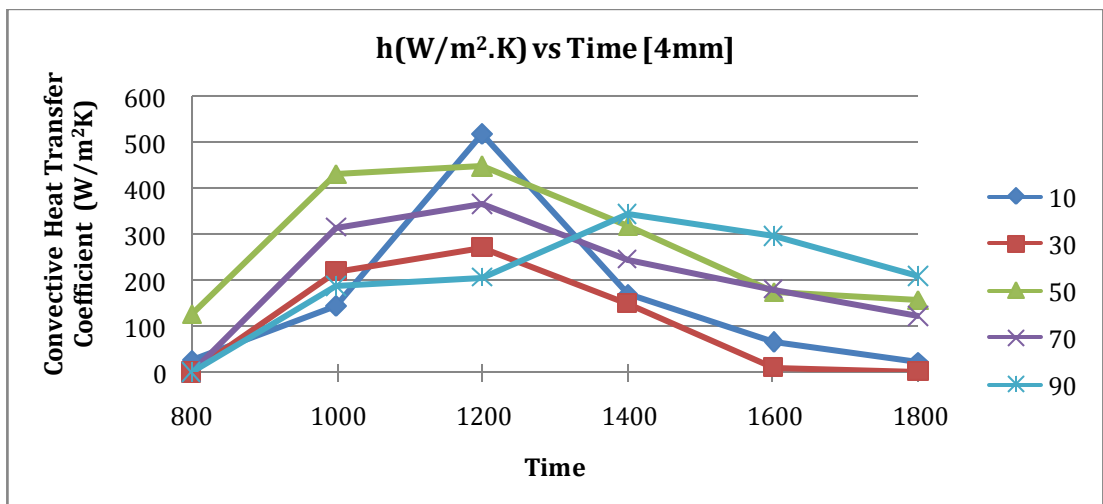


Figure 4.10 Convective heat transfer coefficient for 4mm pinned plate

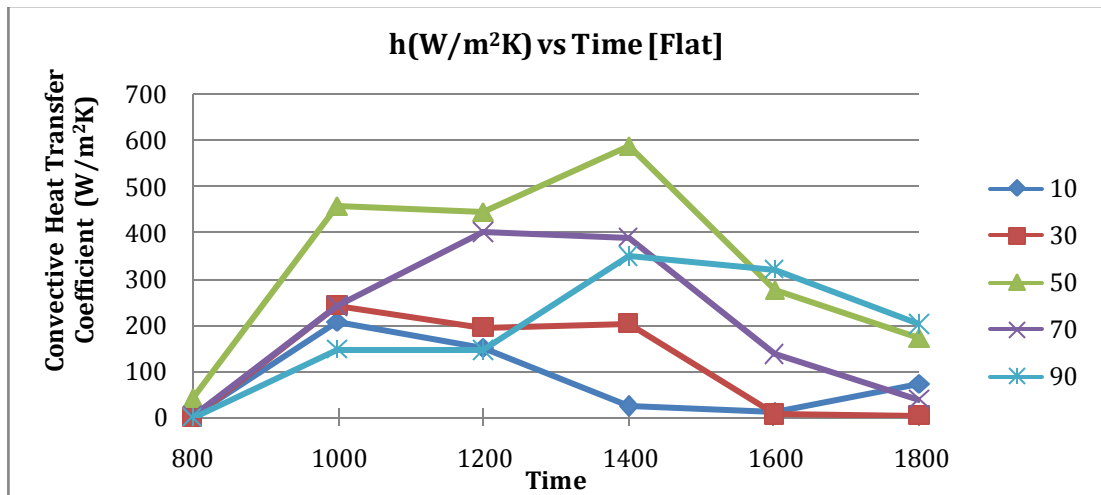


Figure 4.11 Convective heat transfer coefficient for flat plate absorber

In most cases, the wind has greater impact on lower inclination angle configuration such as 10°. This is because when the air passage is more parallel to the direction of wind itself, the wind is able to travel freely inside the channel. It thus, is displacing more hot air with cooler ambient temperature which resulted in lower heat transfer rate. Lower angle configuration may be good in terms of absorbing solar radiation but poor in transferring heat. Instead, for higher inclination angle configuration such as 90°, because the absorber plate is not facing the solar radiation source, which in this case is the Sun, thus the solar insolation is lower compared to another configuration. But because it is perpendicular to the direction of wind, the hot air remains inside the channel or is less displaced by cooler ambient air. However, the heat transfer rate is still lower because of lower solar insolation.

Therefore, the best configuration in this case as presented by the graphs above would be 50° inclination angle since it has the best position for higher solar radiation absorption and lower displacement of hot air by incoming wind. This proves the theory that stated the optimum inclination angle for heat transfer is 45°.

While the effect of different **height of the pins** or types of absorber plates on heat transfer rate can be observed through **Figure 4.12, 4.13, 4.14, 4.15** and **4.16**. The following graphs show the heat transfer rate for 2mm, 3mm, and 4mm pinned plate and flat plate absorber at each configuration.

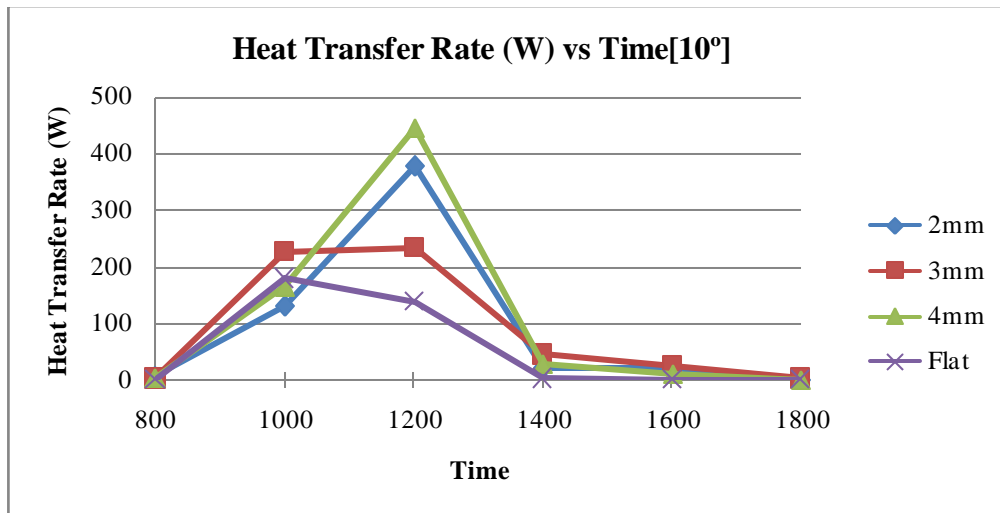


Figure 4.12 Heat transfer rate for different absorber types at 10° inclination angle

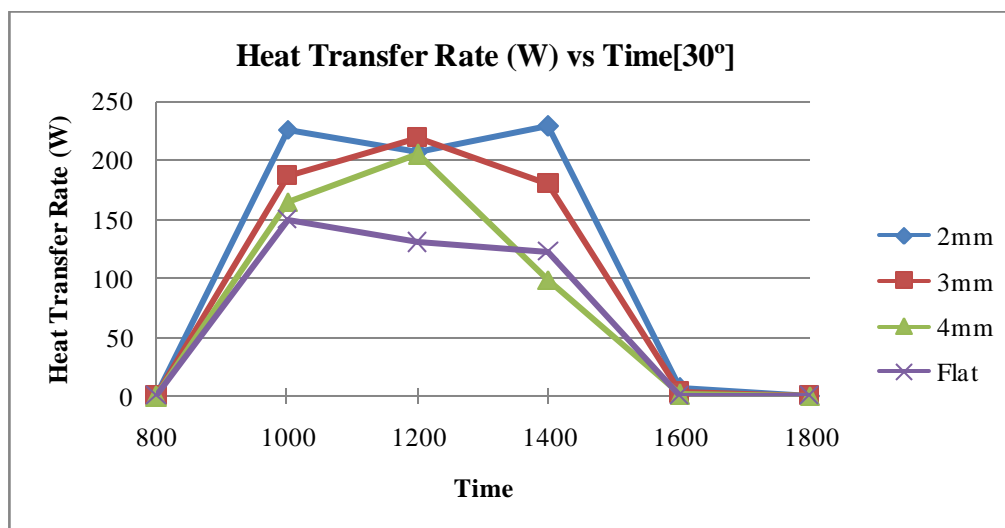


Figure 4.13 Heat transfer rate for different absorber types at 30° inclination angle

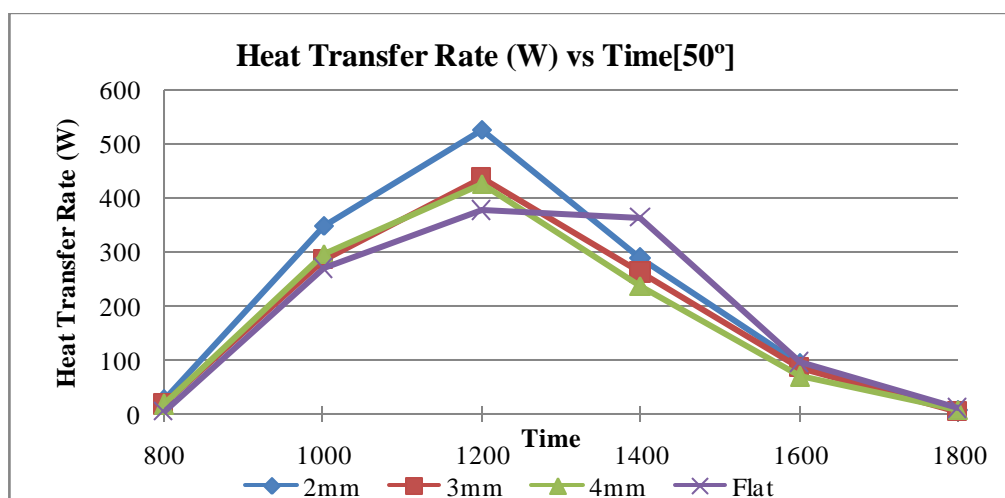


Figure 4.14 Heat transfer rate for different absorber types at 50° inclination angle

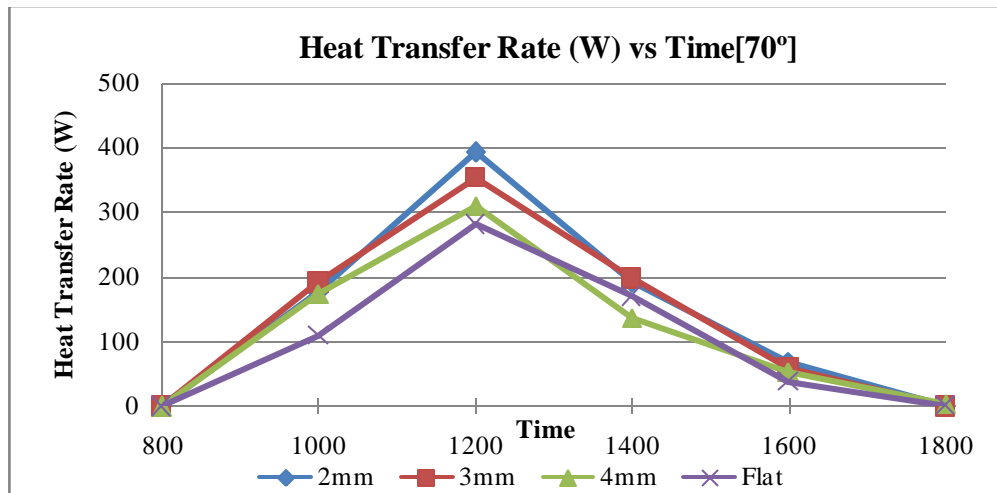


Figure 4.15 Heat transfer rate for different absorber types at 70° inclination angle

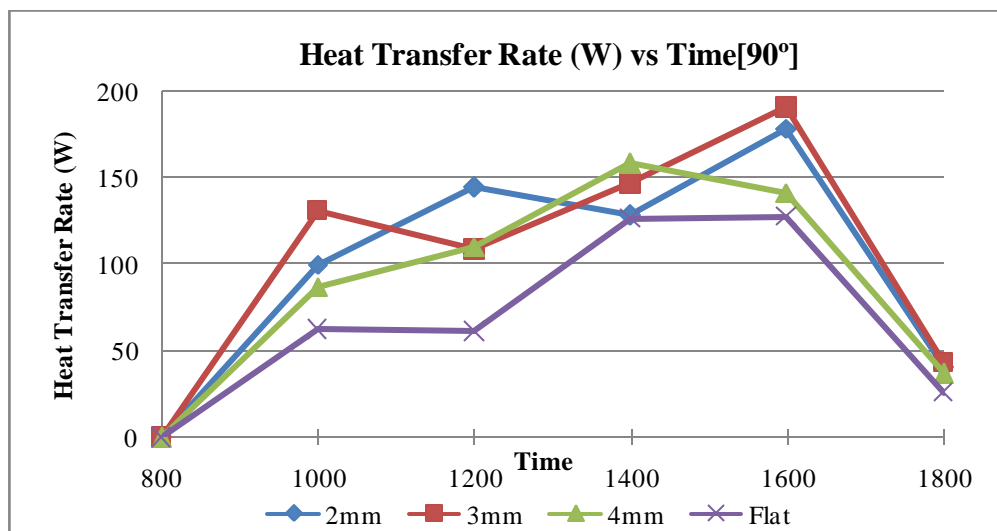


Figure 4.16 Heat transfer rate for different absorber types at 90° inclination angle

It is observed earlier that the air outlet temperature is the highest for system with 2mm pinned absorber plate followed by 3mm and 4 mm plates and lastly the system with flat plate absorber. Heat transfer rate which is influenced by the change in temperature of absorber and inner glazing cover, thus highest for 2mm pinned plate and lowest in flat plate absorber.

In overall, from the graphs plotted for heat transfer rate against time for different types of absorber plate above, it shows that the rate of heat transfer is the highest for 2mm pinned plate followed closely by 3mm and 4 mm pinned plate but noticeably lowest heat transfer rate using flat plate absorber. Even though, inside all the pinned plates channel the boundary layer will be disturbed due to the existence of

pins as resistance, but 2 mm high is thick enough to disturb the air flow which is the reason that explain why it provides the best heat transfer among the 3 pinned plate absorber system. Overall, it can be said that pinned plate absorber can provides higher rate of natural convection heat transfer thus higher efficiency than a typical flat plate. To observe the effect of pinned height or type of absorber plates on air flow behaviour, the following graphs are presented. **Figure 4.17, 4.18, 4.19, 4.20** and **4.21** show the outlet air velocity against time for different type of absorber plates for 10°, 30°, 50°, 70° and 90° inclination angle respectively.

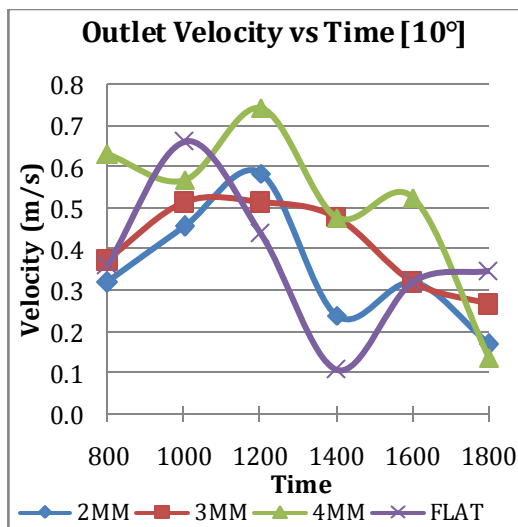


Figure 4.17 Air outlet velocity profile for 10° inclination angle

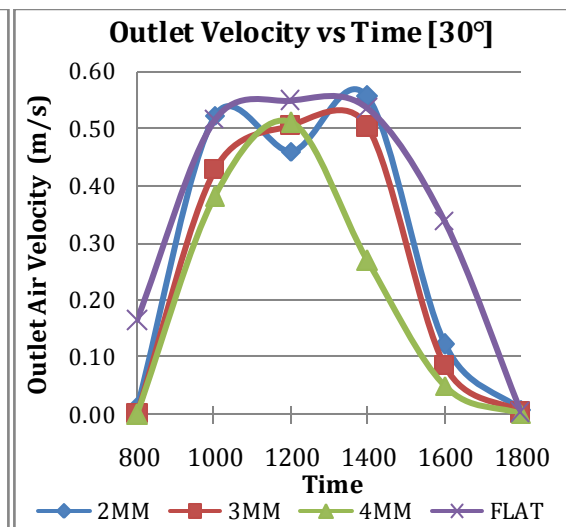


Figure 4.18 Air outlet velocity profile for 30° inclination angle

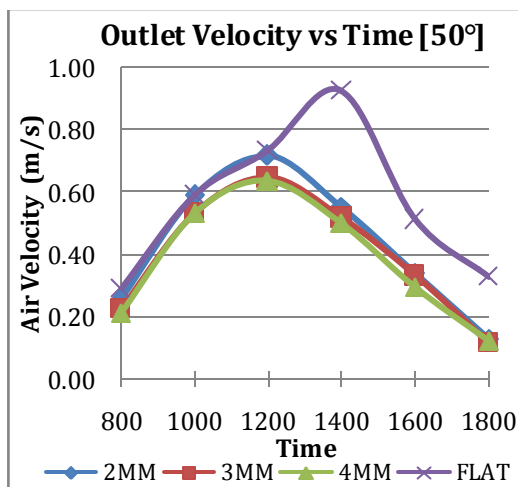


Figure 4.19 Air outlet velocity profile for 50° inclination angle

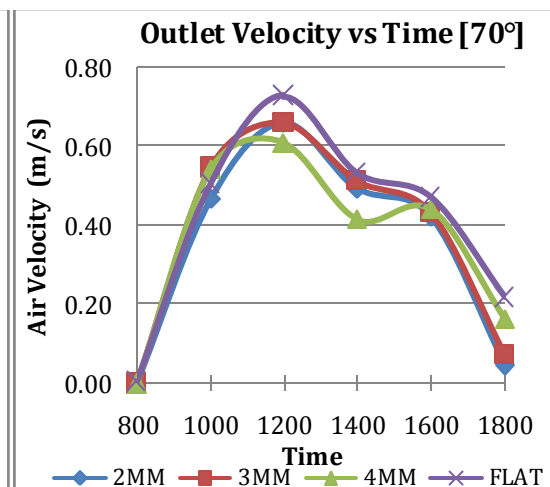
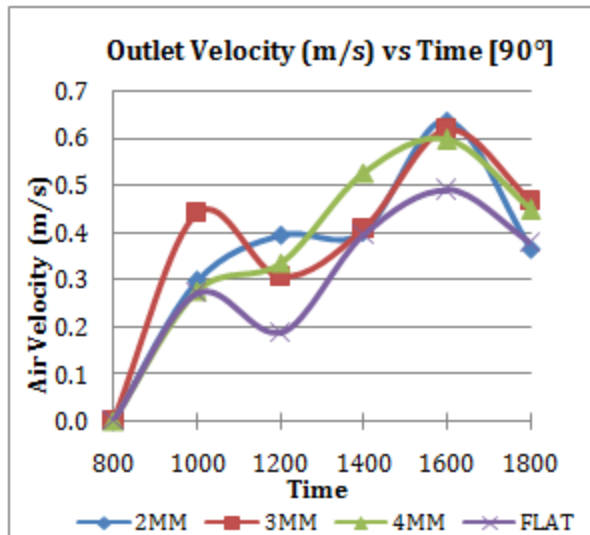


Figure 4.20 Air outlet velocity profile for 70° inclination angle



It can be observed that for the graphs, the variation in air outlet velocity is very unstable. The rank for outlet velocity from highest to lowest is not constant and keeps changing for each configuration. However, the most noticeable result is that the system with flat plate absorber is having the highest air outlet velocity most of the time.

Figure 4.21 Air outlet velocity profile for 90° inclination angle

For flat plate, the boundary layer is not disturbed thus the air flow inside the channel can be higher than pinned plates absorber as it have no resistance. Thus, for the air outlet velocity, it is the lowest in 4mm pinned plate channel as the pins provided the higher resistance for air flow inside the channel than other pinned and flat plates.

To investigate influence of absorber plate types either pinned or flat plate on Reynolds number (Re), the following graphs have been plotted as in **Figure 4.22, 4.23, 4.24, 4.25** and **4.26**. Reynolds number determines the type of air flow behaviour inside the channels.

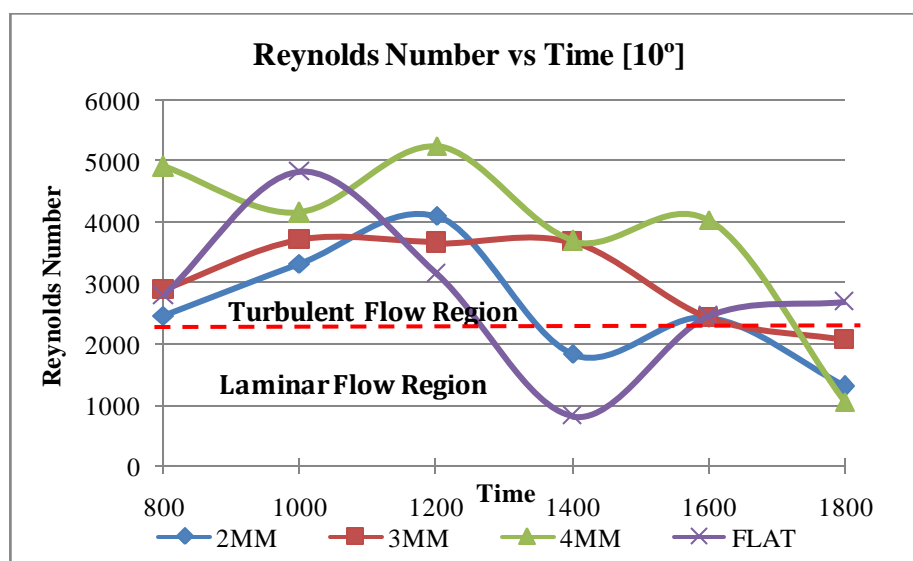


Figure 4.22 Reynolds no. against time at 10° inclination angle

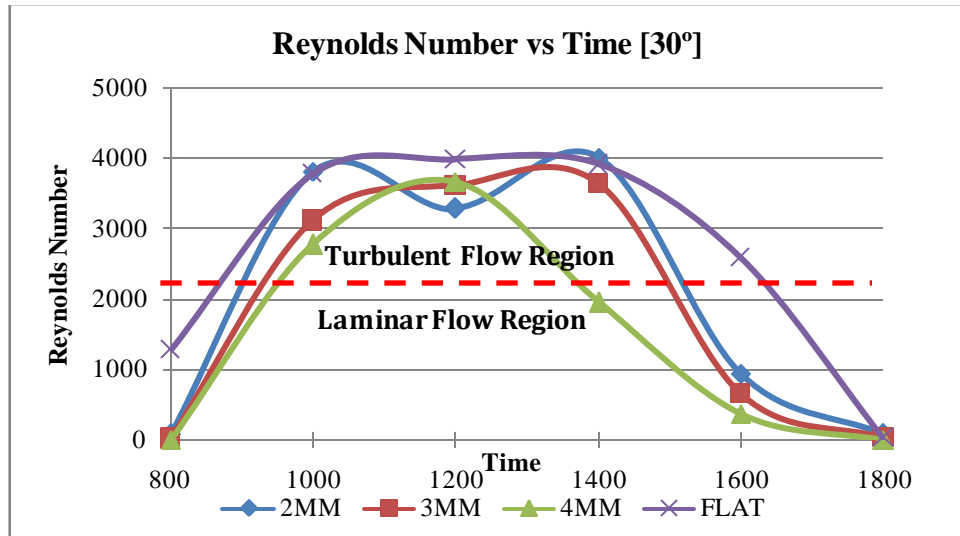


Figure 4.23 Reynolds no. against time at 30° inclination angle

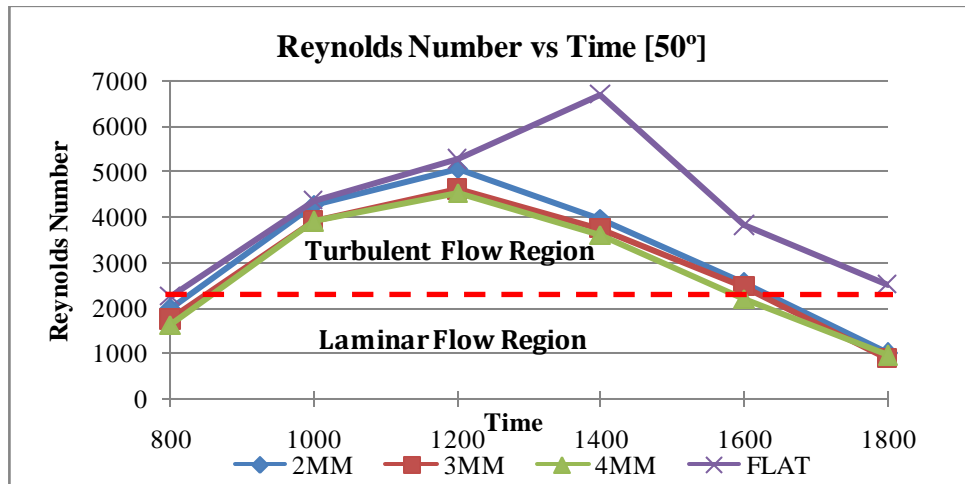


Figure 4.24 Reynolds no. against time at 50° inclination angle

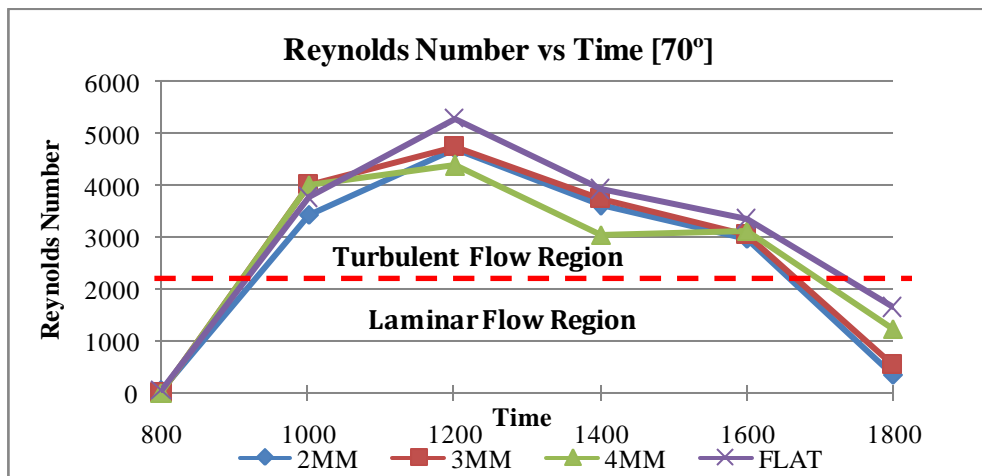


Figure 4.25 Reynolds no. against time at 70° inclination angle

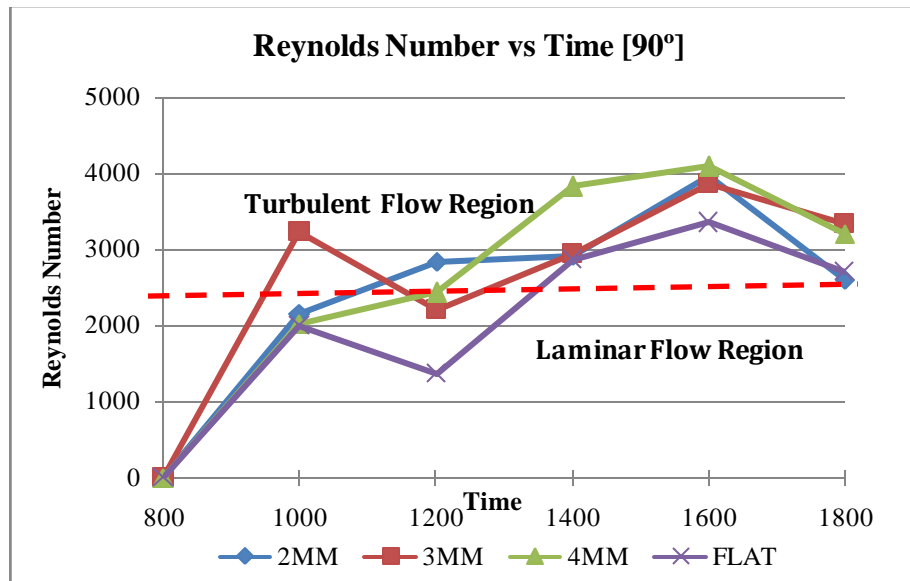


Figure 4.26 Reynolds no. against time at 90° inclination angle

These graphs show that at most of the time for all systems either with pinned or flat plate absorber, the Reynolds number is always more than 2300 throughout the day thus the air flow inside the channel is **turbulent flow**. Since the velocity is highest for flat plate thus the Reynolds number is also highest. But it is uncertain that it has the highest turbulent quantities because the flat plate has less resistance thus fewer disturbances on the boundary layer. Nusselt no. which is proportional with heat transfer is lowest for flat plate. Because the ambient cooler air can quickly passed through a flat plate, thus the heat from the hot absorber surface cannot be transfer effectively to the cooler air.

However, start with 2mm pinned, the boundary layer start to be disturbed due to the resistance from the pins and slower down the velocity of cooler air passing through the channel .Thus it give more time for heat transfer between the medium. The heat transfer which is highest for 2mm pinned plate proven that the turbulence effect is high enough with just 2mm high of resistance. Thus, added turbulence on the surface enhance the heat transfer but it optimum only at certain surface roughness.

It is also observed from the analysis made, the Nusselt number profile is closely matched with the heat transfer rate profile in term of both effects of inclination angle and absorber types. The Nusselt number is increasing in rank of 2mm, 3mm, 4mm pinned and flat plate absorber. Even though this experiment is

claimed as natural convection heat transfer but to validate the claim, the results have to be analyzed further using the following correlations. For free or natural convection, the criterion in Eq. (3.1) must be satisfied.

$$\frac{Gr}{Re^2} > 10$$

However, referring to **Table 4.4** the criterion is not satisfied by the systems at all configurations thus it is not a free convection as $(Gr / Re^2) < 1$

Reynolds number in this case, is observed to have average value around 10^3 and $GrPr (D_h/L)$ is around 10^4 to 10^5 thus reading from Figure 3.4 and 3.5 the systems seems to possess **mixed convection, turbulent flow behaviour** as it can be free convection but sometimes go to the forced convection. A large Reynolds number implies a large forced-flow-velocity and hence less influence of free convection current. The larger the product of Grashof-Prandtl number, the more one would expect free convection effect to prevail.

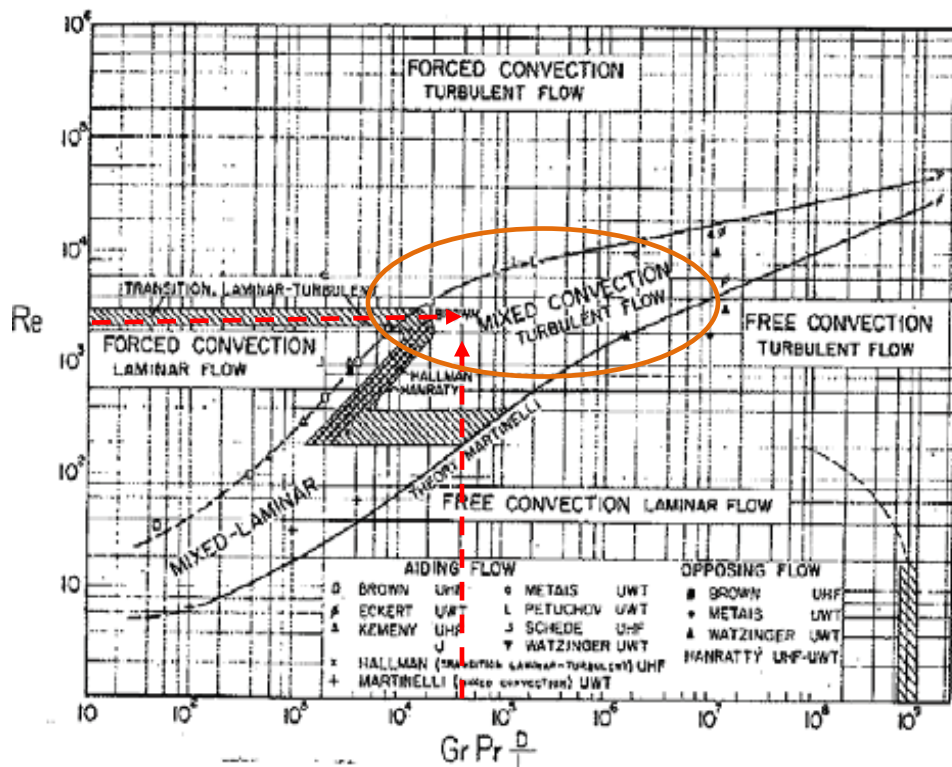


Figure 3.4 Regime of free, forced and mixed convection in vertical tube

Figure 4.27 below represents the relationship between Nusselt number and Rayleigh number, randomly chosen at 50° inclination angle.

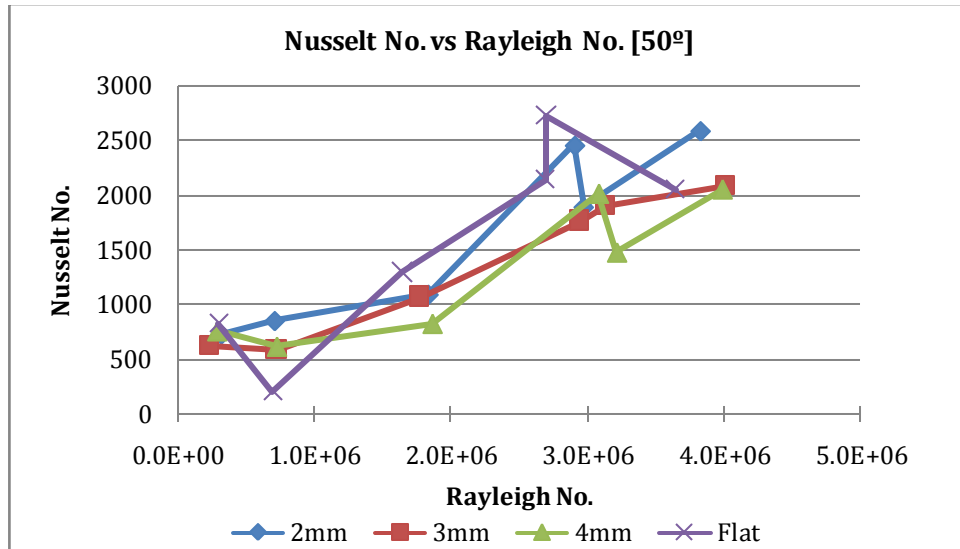


Figure 4.27 Relationship between Nu and Ra at 50° inclination angle

Table 4.4 below shows the comparison on Nusselt no. calculated using different correlations.

Table 4.4 Comparison on Nusselt number of different correlations at 12pm

Type	Angle	Gr/Re ²	Re	GrPr (Dh/L)	Nu ^[1]	Nu ^[2]	% error	Nu ^[3]	% error
2MM	10°	0.263	4.10E+03	1.95E+05	2175.42	44.18	97.97	22.837	98.95
	30°	0.395	3.29E+03	1.90E+05	1285.44	41.56	96.77	22.663	98.24
	50°	0.205	5.08E+03	2.34E+05	2591.82	47.43	98.17	23.894	99.08
	70°	0.215	4.71E+03	2.12E+05	2176.92	46.14	97.88	23.294	98.93
	90°	0.366	2.85E+03	1.32E+05	1335.28	38.97	97.08	20.691	98.45
3MM	10°	0.439	3.66E+03	2.61E+05	1051.68	43.73	95.84	24.540	97.67
	30°	0.341	3.63E+03	1.99E+05	1314.84	42.81	96.74	22.933	98.26
	50°	0.260	4.62E+03	2.45E+05	2082.44	46.37	97.77	24.174	98.84
	70°	0.240	4.74E+03	2.39E+05	1765.18	46.61	97.36	24.013	98.64
	90°	0.642	2.21E+03	1.39E+05	950.36	36.54	96.16	20.979	97.79
4MM	10°	0.176	5.24E+03	2.14E+05	2357.91	47.52	97.98	23.361	99.01
	30°	0.328	3.67E+03	1.96E+05	1248.82	42.90	96.56	22.844	98.17
	50°	0.266	4.55E+03	2.44E+05	2049.46	46.18	97.75	24.143	98.82
	70°	0.261	4.38E+03	2.22E+05	1675.14	45.41	97.29	23.580	98.59
	90°	0.542	2.44E+03	1.43E+05	954.56	37.58	96.06	21.113	97.79
FLAT	10°	0.552	3.15E+03	2.43E+05	697.47	41.78	94.01	24.107	96.54
	30°	0.255	3.99E+03	1.80E+05	895.79	43.62	95.13	22.366	97.50
	50°	0.181	5.27E+03	2.23E+05	2053.13	47.75	97.67	23.599	98.85
	70°	0.152	5.29E+03	1.88E+05	1847.91	47.23	97.44	22.625	98.78
	90°	1.370	1.37E+03	1.14E+05	666.25	31.65	95.25	19.951	97.01
						Mean % error	96.84	Mean % error	98.30

Since at 12 noon the effects of the variables on the investigated parameters in this experiment are more noticeable, thus it has been selected for Nusselt number validation purpose. $Nu^{[1]}$ is the Nusselt number calculated using Eq. (2.3), $Nu^{[2]}$ is from Eq. (3.5) for mixed convection; turbulent flow region as in Figure 3.5 and $Nu^{[3]}$ is from Eq. (3.6) for natural convection. The percentage error has been calculated by comparing to the main Nusselt number calculated in this project which is $Nu^{[1]}$ to $Nu^{[2]}$ and $Nu^{[3]}$. The error is exceptionally large which the mean % error between $Nu^{[1]}$ and $Nu^{[2]}$ is **96.84%** and slightly higher for $Nu^{[3]}$ which is **98.30 %**.

Natural convection is too complex and normally the error can be acceptable up to 25%. However, in this case the error is exceedingly higher but there are for reasons. Since correlation for $Nu^{[2]}$ is specified for horizontal tubes it does not take into account the effect of inclination angle as well as the type of the channel which in this project is a rectangular duct. It is specified for mixed convection, turbulent flow. Also, for $Nu^{[3]}$ correlation, it is too general which only takes into account the influence of Rayleigh number. Based on the results, it shows that inclination angle plays a very big role in heat transfer either free or forced or mixed convection. In addition, in this project the absorber plates are introduced with pins of different heights that also have pretty much impact on the air stream velocity thus heat transfer rate which is proportional with the Nusselt number. Nusselt number which is greatly affected by the change in temperatures between surfaces due to effect of inclination angle and absorber types caused huge difference between correlations that disregarded these important variables with the one that implies.

CHAPTER 5

CONCLUSION

The objectives of this project have been fully achieved. The effect of inclination angle on the outlet temperature, solar insolation as well as convective heat transfer has been determined. At lower inclination angle, the intensity of solar insolation is higher since in that position the absorber plates received more incident of solar radiation from the sunlight. Yet, the impact of wind of the system is much greater at lower inclination angle as the position is about parallel to the direction of ambient wind thus allow the cooler ambient air to freely enter the channel and displaced the hot air inside the channel. This explained the reason for optimum inclination angle that would provides best convective heat transfer should be about 45° since the more solar radiation can be absorbed and impact of wind is reduced. The results from the experimental works proven this reasoning as the heat transfer rate are higher when the system is at 50° inclination angle. The effect of types of absorber plates on the heat transfer rate and outlet temperature has been studied which noticeably higher for pinned plates than a normal flat plate absorber. In addition, heat transfer rate is the highest for the system with 2mm pinned plate absorbers subsequently followed by system with 3mm and 4mm pinned plate absorbers and always lowest for flat plate absorber. For outlet temperature profile, it closely matched with insolation profile and shows higher value for shorter pins yet still higher compared to normal flat plate absorber. Air outlet velocity in the other hand is higher for system with flat plate than pinned plates as it does not give any resistance to the air stream flow as the pinned plates did. For outlet temperature profile, it closely matched with insolation profile and shows higher value for shorter pins yet still higher compared to normal flat plate absorber. The boundary layer is disturbed in channel with pinned plate thus the effect of added turbulent enhance the heat transfer. The fluid flows inside the channels indeed are turbulent but the claim of free convection is denied as the systems do not satisfy the criterion for a free convection. Instead, it shows a mixed convection, turbulent flow behaviour which sometimes can reach forced convection.

4.1 Recommendations

In this section, several recommendation and modification are suggested to prepare a better experimental setup thus better result. Firstly, the major problems identified in the experimental work in this project are the ineffective method of data collection which will affect the accuracy and precision of the reading. Ideally experiment should be conducted as the following suggestion in order to obtain more consistent readings:

- i. Solarimeter which is the device used to measure the solar insolation is a real time measuring device. To measure the solar insolation for every five minutes in order to consider the average reading is quite tedious. Thus if data logger for solar insolation with automatic recording capability is available, the measurement for the insolation would be more accurate and reliable.
- ii. Use better or more sensitive instrumentation for measuring the air flow velocity as it is one of the important parameters investigated. Earlier, when the anemometer is used it always gave zero reading for the ambient wind velocity as well as the outlet velocity for air coming out from the channels due to lack of sensitivity. By using the flow sensor, it measured the velocity in term of voltage, thus need a conversion factor to convert the voltage in volt to velocity in m/s. Up to date there is no standard conversion factor for this parameters. The one used in this analysis is the one governed by the design specification of the flow sensor which unable be proven as accurate. To obtained better and more accurate result, correct instrumentation must be used to measure the air flow velocity.

While for the physical model itself, few modifications should be amend in order to yield better result. The technical work which involved the staggered pinned absorber plates production at the different height, it is recommended to have them custom made by a reliable punching machine. By preparing them manually, the force exerted onto the puncher might not be constant thus resulted pinned may not have the same height as required along the absorber plates. This is the main reason why the results fluctuated a lot among the pinned plate absorbers.

Besides that, it is also mentioned that wind is greatly affecting the data measurement. Therefore, test rig should be improved with special inlet and outlet designs in order to reduce the impact of wind onto the system. Also, because of the weather is frequently changed since it was conducted in rainy season, the results obtained in this experiment are totally affected thus reduces the reliability and accuracy. For future experimental work, it is suggested to conduct the experiment in better times preferably on January to October.

For future works, the experiment should be expanded not only to staggered pinned plate but parallel pinned plate and double-sided pinned plate absorber as well to investigate better convective heat transfer behaviour. Also, the continuation of this project should involve the investigation on the effect of channel length on the parameters of interest which was suggested at first but unable to execute due to limitation of time.

4.2 Relevancy to the Objectives

All the activities conducted and completed throughout the project time frame are basically according to the requirement of this project. Each of the objectives is properly translated into experimental works which are then conducted to collect the necessary data to investigate the project interest as guided by the objectives. The results obtained from the experimental works satisfied the objectives and proven some reasoning as discussed in literature review section. In overall, the project is fully completed in right track.

REFERENCES

- [1] Shafiee, S., Topal, E. (2009). “When will fossil fuel reserves be diminished?” *Energy Policy*, vol. 37, pp. 181-189.
- [2] Kalogirou, S. A. (2004). *Solar Thermal Collectors and Applications*. Mechanical Engineering, Higher Technical Institute, Cyprus.
- [3] (n.d). Stack Ventilation and Bernoulli’s Principle. In Autodesk *Education Community-Sustainability Workshop*. Retrieved December 10, 2012, from <http://sustainabilityworkshop.autodesk.com/fundamentals/stack-ventilation-and-bernoullis-principle>.
- [4] (n.d). Indirect Solar Gain System. In *California Energy Commission: Consumer Energy Center*. Retrieved December 10, 2012, from <http://www.consumerenergycenter.org/home/construction/solardesign/indirect.html#top>.
- [5] (n.d). Solar Air Heat. In *Wikipedia*. Retrieved December 10, 2012, from http://en.wikipedia.org/wiki/Solar_air_heat.
- [6] Andren, L. (2003). *Solar Insolation: Practical Applications for the Built Environment*. James & James Publisher, p. 4.
- [7] Nielsen, R. (2005). Solar Radiation. In *The Nielsen’s Website*. Retrieved June, 30, 2012, from <http://home.iprimus.com.au/nielsens/solrad.html>
- [8] (2010) European Journal of Scientific Research, EuroJournals Publishing, Inc. vol. 40, No. 1, pp. 144-155. Retrieved June, 30, 2012 from <http://www.eurojournals.com/ejsr>.
- [9] Y.Varol, H. F. Oztop and A.Varol (2006). “Effects of Thin Fin on Natural Convection in Porous Triangular Enclosures.”
- [10] Incropera, F.P., Dewitt, D. P., Bergman T. L. and Lavine, A. S. (2007) “Introduction to Heat Transfer,” John Wiley & Sons (Asia) Pte Ltd, 5th Ed., pp. 551-554.

- [11] Turns, S. R. (2006). "Thermal- Fluid Sciences: An Integrated Approach," Cambridge University Press.
- [12] Hollands, K. G. T., Unny. S. E., Raithbay. G. D., and Konicek. L. (1976) "Free Convection Heat Transfer Across Inclined Air Layer," *J. Heat Transfer*, 98, 189,
- [13] Ayyaswamy, P. S., and Calton. I. (1973). "The Boundary Layer Regime for Natural Convection in a Differentially Heated, Tilted Rectangular Cavity," *J. Heat Transfer*, 95, 543.
- [14] Catton, I., "Natural Convection in Enclosure," *Proc. 6th Int. Heat Transfer Conf.*, Toronto, Canada, 1978, Vol. 6, pp. 13-31.
- [15] MacGregor, R. K., and A.P. Emery (1969), "Free Convection through Vertical Plane Layers: Moderate and High Prandtl Number Fluids," *J. Heat Transfer*, 91, 391.
- [16] Premalata, M., Priya, S. S., Saravanakumaar, A., "Experimental Investigation of Inclination Angle on Heat Transfer Characteristics of Wickless Solar Heat Pipe".
- [17] Matuszewki, P., Sawicka M. (2010). *Optimization of Solar Air Collector*. School of Energy and Science, Aalborg University, Denmark.
- [18] Toh, S. P. (2011). "Analytical and Experimental Investigation of Convective Heat Transfer in Solar Collector," Universiti Teknologi PETRONAS, Malaysia.
- [19] Serkayaa, A. A., Bilirb, S., Kargicib, S., "Experimental Investigation of the Effects of Orientation Angle on Heat Transfer Performance of Pin-Finned Surfaces in Natural Convection."
- [20] Bashria, A. A. Y., Adam, N. M., "Performance Analysis of Single and Double Passes Flat Plate Collector With and Without Porous Media."
- [21] Krogstad, P. A., Antonia, R. A. (1999), "Surface Roughness Effects on Turbulent Boundary Layer". University of Newcastle, Newcastle, Australia.

- [22] R. Karthikeyan et. al, *International Journal of Advanced Engineering Sciences and Technologies*. Vol. 10, Issue No. 1, 125 – 138.
- [23] Boelter, L. M. K., Leasure, R., Romie, F. E., Sanders, V. D., Elswick, W. R., Young, G., A.(1950). *Experimental Determination of Thermal and Hydrodynamics Behaviour of Flowing Air along Finned Plates*.
- [24] Brigham, B. A., and VanFossen, G. J. (1984). “Length to Diameter Ratio and Row Number Effects in Short Pin Fin Heat Transfer,” *Journal of Heat Transfer*, vol. 106, pp. 241-245.
- [25] Armstrong, J., Winstanley, D. (1988) “A Review of Staggered Array Pin Fin Heat Transfer for Turbine Cooling Applications,” *Journal of Turbomachinery*, vol.110, pp. 94-103.
- [26] Holman, J. P. (2010) “Combined Free and Forced Convection,” *Heat Transfer*, 10th Edition, pp. 358-360, McGraw Hill Education.
- [27] Metais, B., and E. R. G. Eckart. (1964). “Forced, Mixed and Free Convection Regimes,” *J. Heat Transfer*, ser. C, vol. 86, p. 295.
- [28] Brown, C. K., Gavin, W. H. (1955). “Combined Free and Forced Convection, I, II,” *Can. J. Chem. Eng.*, vol. 43, no. 6, p. 361.
- [29] Lloyd, J. R., Moran, W. R. (1974). “Natural Convection Adjacent to Horizontal Surface of Various Platforms,” *Journal of Heat Transfer*, 96, pp. 443-447.

APPENDICES

**APPENDIX I: RAW DATA COLLECTED FROM EXPERIMENTAL
WORKS**

APPENDIX II: ANALYZED DATA

Table I.1 Raw data for 10° degree inclination angle

TIME	T _{G1} (°C)	T _{G2} (°C)	T _A (°C)	T _{amb} (°C)	T _{out} (°C)	T _{mean} (°C)	ΔT (°C)	V _{wind} (m/s)	Air Flow _{outlet} (V)	V _{out} (m/s)	Insolation (W/m ²)
2MM STAGGERED PINNED PLATE ABSORBER											
08:00	27.40	28.22	30.92	26.00	26.63	26.32	0.63	0.200	1.032	0.318	102.33
10:00	57.15	62.23	68.90	33.00	40.47	36.74	7.47	2.000	1.055	0.454	638.00
12:00	56.32	61.97	67.27	35.00	52.20	43.60	17.20	1.800	1.077	0.583	753.00
14:00	26.28	31.14	32.75	26.50	28.67	27.59	2.17	0.633	1.059	0.239	482.02
16:00	27.26	31.46	33.72	27.80	29.43	28.62	1.63	0.300	1.032	0.318	73.00
18:00	24.89	26.13	27.35	25.50	25.53	25.52	0.03	0.200	1.035	0.168	55.51
3MM STAGGERED PINNED PLATE ABSORBER											
08:00	27.33	28.98	31.73	26.00	26.23	26.12	0.23	0.200	1.041	0.371	102.33
10:00	50.42	65.45	71.03	33.00	44.53	38.77	11.53	2.000	1.065	0.513	638.00
12:00	56.01	66.31	71.23	35.00	46.98	40.99	11.98	1.800	1.065	0.513	753.00
14:00	26.12	31.62	32.98	26.50	28.88	27.69	2.38	0.633	1.059	0.477	482.02
16:00	27.15	32.17	34.00	27.80	29.93	28.87	2.13	0.300	1.032	0.318	73.00
18:00	24.73	26.37	27.36	25.50	25.78	25.64	0.28	0.300	1.023	0.265	55.51
4MM STAGGERED PINNED PLATE ABSORBER											
08:00	26.85	28.21	31.60	26.00	26.20	26.10	0.20	0.200	1.085	0.630	102.33
10:00	55.26	65.00	71.02	33.00	40.55	36.78	7.55	2.000	1.075	0.569	638.00
12:00	55.71	63.50	68.50	35.00	50.87	42.94	15.87	1.800	1.104	0.742	753.00
14:00	26.50	30.79	32.59	26.50	28.10	27.30	1.60	0.633	1.059	0.477	482.02
16:00	29.52	31.77	33.57	27.80	28.38	28.09	0.58	0.300	1.067	0.524	73.00
18:00	25.28	26.43	27.44	25.50	25.78	25.64	0.28	0.300	1.001	0.136	55.51
FLAT PLATE ABSORBER											
08:00	27.10	28.36	29.71	26.00	25.48	25.74	-0.52	0.200	1.039	0.359	102.33
10:00	53.49	59.80	62.42	33.00	40.08	36.54	7.08	2.000	1.09	0.660	638.00
12:00	52.96	63.77	66.53	35.00	43.35	39.18	8.35	1.800	1.052	0.436	753.00
14:00	26.21	28.46	30.44	26.50	27.15	26.83	0.65	0.633	1.050	0.106	482.02
16:00	28.46	30.65	32.76	27.80	27.95	27.88	0.15	0.300	1.032	0.318	73.00
18:00	25.08	25.84	26.42	25.50	25.65	25.58	0.15	0.300	1.154	0.346	55.51

Table I.2 Raw data for 30° degree inclination angle

TIME	T _{G1} (°C)	T _{G2} (°C)	T _A (°C)	T _{amb} (°C)	T _{out} (°C)	T _{mean} (°C)	ΔT (°C)	V _{wind} (m/s)	Air Flow outlet (V)	V _{out} (m/s)	Insolation (W/m ²)
2MM PINNED PLATE ABSORBER											
08:00	28.26	30.02	33.10	26.33	27.63	26.98	1.30	0.68	0.980	0.01	121.42
10:00	43.53	52.47	59.13	31.88	43.08	37.48	11.20	0.50	1.067	0.52	368.70
12:00	46.32	55.57	62.63	34.75	46.58	40.66	11.83	1.05	1.056	0.46	665.83
14:00	45.70	52.46	59.20	33.63	44.35	38.99	10.73	2.30	1.073	0.56	502.93
16:00	28.29	31.12	32.41	27.65	29.04	28.34	1.39	1.33	0.999	0.12	115.28
18:00	24.43	25.66	26.38	24.43	25.73	25.08	1.30	0.10	0.980	0.01	3.54
3MM PINNED PLATE ABSORBER											
08:00	28.09	31.05	34.03	26.33	27.19	26.76	0.87	0.68	0.979	0.00	121.42
10:00	46.32	55.21	60.91	31.88	43.18	37.53	11.31	0.50	1.051	0.43	368.70
12:00	48.81	58.30	63.18	34.75	46.12	40.43	11.37	1.05	1.064	0.51	665.83
14:00	46.53	54.35	59.27	33.63	42.93	38.28	9.30	2.30	1.064	0.50	502.93
16:00	28.08	31.14	32.02	27.65	28.63	28.14	0.98	1.33	0.993	0.09	115.28
18:00	24.33	25.73	26.20	24.43	25.13	24.78	0.70	0.10	0.979	0.00	3.54
4MM PINNED PLATE ABSORBER											
08:00	28.45	29.89	33.09	26.33	27.73	27.03	1.41	0.68	0.978	0.00	121.42
10:00	45.48	53.00	59.94	31.88	43.11	37.49	11.23	0.50	1.043	0.38	368.70
12:00	51.76	55.75	62.36	34.75	45.24	40.00	10.49	1.05	1.065	0.51	665.83
14:00	47.84	51.33	58.05	33.63	43.18	38.40	9.55	2.30	1.024	0.27	502.93
16:00	28.60	30.94	31.85	27.65	28.43	28.04	0.78	1.33	0.987	0.05	115.28
18:00	24.97	25.78	26.32	24.43	25.53	24.98	1.10	0.10	0.978	0.00	3.54
FLAT PLATE ABSORBER											
08:00	28.59	29.72	31.21	26.33	26.34	26.33	0.01	0.68	1.006	0.16	121.42
10:00	47.21	51.90	54.02	31.88	39.39	35.63	7.52	0.50	1.066	0.52	368.70
12:00	49.17	55.06	57.79	34.75	40.92	37.84	6.17	1.05	1.071	0.55	665.83
14:00	45.08	52.30	54.57	33.63	39.56	36.59	5.94	2.30	1.069	0.54	502.93
16:00	26.38	30.44	30.80	27.65	27.70	27.67	0.05	1.33	1.035	0.34	115.28
18:00	24.37	25.52	25.88	24.43	25.08	24.76	0.65	0.10	0.979	0.00	3.54

Table I.3 Raw data for 50° degree inclination angle

TIME	T _{G1} (°C)	T _{G2} (°C)	T _A (°C)	T _{amb} (°C)	T _{out} (°C)	T _{mean} (°C)	ΔT (°C)	V _{wind} (m/s)	Air Flow Outlet (V)	V _{out} (m/s)	Insolation (W/m ²)
2MM PINNED PLATE ABSORBER											
08:00	27.05	29.16	31.87	26.43	28.92	27.67	2.49	0.23	1.021	0.25	154.30
10:00	45.64	50.68	56.36	29.21	44.57	36.89	15.36	1.00	1.078	0.59	368.73
12:00	57.55	61.68	69.81	32.51	51.93	42.22	19.41	0.65	1.100	0.72	630.38
14:00	49.85	54.42	60.29	32.70	46.33	39.52	13.63	1.10	1.072	0.55	527.70
16:00	39.04	42.94	45.67	30.41	37.36	33.89	6.95	1.93	1.036	0.34	328.67
18:00	27.01	28.28	29.16	26.33	28.20	27.26	1.88	0.05	1.000	0.13	7.05
3MM PINNED PLATE ABSORBER											
08:00	26.15	28.07	31.60	26.43	28.38	27.40	1.95	0.23	1.016	0.23	154.30
10:00	45.40	51.60	56.86	29.21	43.08	36.15	13.88	1.00	1.068	0.53	368.73
12:00	56.89	62.90	69.88	32.51	50.24	41.38	17.73	0.65	1.088	0.65	630.38
14:00	49.20	56.74	59.60	32.70	45.88	39.29	13.18	1.10	1.066	0.52	527.70
16:00	38.54	42.80	45.12	30.41	37.17	33.79	6.76	1.93	1.034	0.33	328.67
18:00	26.92	28.12	28.36	26.33	27.65	26.99	1.33	0.05	0.998	0.11	7.05
4MM PINNED PLATE ABSORBER											
08:00	27.32	29.07	31.75	26.43	28.60	27.51	2.17	0.23	1.014	0.21	154.30
10:00	48.14	51.49	56.79	29.21	43.64	36.43	14.43	1.00	1.068	0.53	368.73
12:00	57.34	62.36	69.66	32.51	50.11	41.31	17.60	0.65	1.086	0.64	630.38
14:00	49.56	53.40	61.08	32.70	45.11	38.91	12.41	1.10	1.063	0.50	527.70
16:00	38.99	42.07	45.21	30.41	36.46	33.44	6.05	1.93	1.028	0.29	328.67
18:00	27.36	28.32	28.89	26.33	28.13	27.23	1.80	0.05	0.999	0.12	7.05
FLAT PLATE ABSORBER											
08:00	26.86	28.14	30.65	26.43	26.92	26.67	0.50	0.23	1.027	0.29	154.30
10:00	46.48	48.79	52.56	29.21	40.95	35.08	11.75	1.00	1.079	0.59	368.73
12:00	54.66	61.20	64.38	32.51	45.99	39.25	13.48	0.65	1.102	0.73	630.38
14:00	47.93	55.06	56.13	32.70	42.93	37.82	10.23	1.10	1.135	0.93	527.70
16:00	38.09	42.66	43.16	30.41	35.23	32.82	4.82	1.93	1.065	0.51	328.67
18:00	27.10	27.78	28.46	26.33	27.11	26.72	0.78	0.05	1.034	0.33	7.05

Table I.4 Raw data for 70° degree inclination angle

TIME	T _{G1} (°C)	T _{G2} (°C)	T _A (°C)	T _{amb} (°C)	T _{out} (°C)	T _{mean} (°C)	ΔT (°C)	V _{wind} (m/s)	Air Flow _{outlet} (V)	V _{out} (m/s)	Insolation (W/m ²)
2MM PINNED PLATE ABSORBER											
08:00	29.38	30.28	32.67	25.88	28.46	27.17	2.58	0.43	0.978	0.002	38.33
10:00	44.85	47.14	51.45	31.08	40.84	35.96	9.76	1.03	1.058	0.469	343.90
12:00	55.22	57.90	65.82	33.43	49.08	41.25	15.65	1.90	1.090	0.660	526.77
14:00	46.21	49.62	54.13	32.37	42.43	37.40	10.06	1.13	1.062	0.495	224.67
16:00	47.30	51.38	53.58	41.37	45.80	43.59	4.43	1.90	1.050	0.422	215.00
18:00	32.15	33.60	34.19	32.32	33.15	32.74	0.83	0.60	0.99	0.045	10.00
2MM PINNED PLATE ABSORBER											
08:00	28.76	29.98	31.83	25.88	27.69	26.78	1.81	0.43	0.978	0.000	38.33
10:00	44.33	50.10	51.83	31.08	40.17	35.62	9.09	1.03	1.071	0.546	343.90
12:00	55.45	62.00	67.80	33.43	47.48	40.45	14.05	1.90	1.090	0.660	526.77
14:00	45.95	51.47	54.46	32.37	42.35	37.36	9.98	1.13	1.065	0.515	224.67
16:00	46.95	52.33	53.69	41.37	45.05	43.21	3.68	1.90	1.051	0.432	215.00
18:00	32.20	33.13	33.60	32.32	32.40	32.36	0.07	0.60	0.99	0.074	10.00
2MM PINNED PLATE ABSORBER											
08:00	29.62	30.49	32.57	25.88	28.20	27.04	2.32	0.43	0.978	0.000	38.33
10:00	45.45	47.61	51.91	31.08	39.42	35.25	8.34	1.03	1.070	0.544	343.90
12:00	55.39	58.83	65.52	33.43	46.80	40.12	13.38	1.90	1.082	0.611	526.77
14:00	45.95	48.20	53.45	32.37	40.99	36.68	8.62	1.13	1.049	0.416	224.67
16:00	46.69	49.88	51.85	41.37	44.59	42.98	3.22	1.90	1.053	0.442	215.00
18:00	32.83	33.64	34.04	32.32	33.15	32.74	0.83	0.60	1.01	0.165	10.00
2MM PINNED PLATE ABSORBER											
08:00	28.77	29.10	30.65	25.88	26.84	26.36	0.96	0.43	0.979	0.004	38.33
10:00	44.27	45.72	47.50	31.08	36.66	33.87	5.58	1.03	1.064	0.507	343.90
12:00	53.05	56.81	59.40	33.43	43.50	38.46	10.07	1.90	1.102	0.729	526.77
14:00	45.13	48.92	49.52	32.37	40.62	36.50	8.25	1.13	1.069	0.534	224.67
16:00	46.34	49.97	51.09	41.37	43.58	42.48	2.21	1.90	1.058	0.471	215.00
18:00	32.41	33.38	33.74	32.32	32.52	32.42	0.20	0.60	1.015	0.218	10.00

Table I.5 Raw data for 90° degree inclination angle

TIME	T _{G1} (°C)	T _{G2} (°C)	T _A (°C)	T _{amb} (°C)	T _{out} (°C)	T _{mean} (°C)	ΔT (°C)	V _{wind} (m/s)	Air Flow _{outlet} (V)	V _{out} (m/s)	Insolation (W/m ²)
2MM PINNED PLATE ABSORBER											
08:00	30.39	29.56	30.41	26.96	28.52	27.74	1.55	0.30	0.978	0.000	12.00
10:00	47.57	46.45	49.48	31.95	40.77	36.36	8.81	1.20	1.028	0.295	270.00
12:00	49.35	50.05	53.47	33.87	43.43	38.65	9.57	0.30	1.045	0.395	515.00
14:00	47.28	48.15	50.53	33.33	41.65	37.49	8.32	0.30	1.046	0.401	235.00
16:00	59.61	60.23	62.35	44.85	52.42	48.64	7.57	1.20	1.086	0.636	253.00
18:00	42.69	44.73	45.37	39.17	42.08	40.63	2.92	0.30	1.040	0.365	29.00
3MM PINNED PLATE ABSORBER											
08:00	30.58	29.80	30.78	26.96	28.43	27.70	1.47	0.30	0.978	0.00	12.00
10:00	47.56	47.97	50.47	31.95	39.62	35.79	7.67	1.20	1.053	0.44	270.00
12:00	50.18	51.57	54.15	33.87	43.13	38.50	9.27	0.30	1.030	0.31	515.00
14:00	47.60	47.24	49.28	33.33	42.73	38.03	9.40	0.30	1.047	0.41	235.00
16:00	59.44	58.61	61.14	44.85	53.18	49.01	8.33	1.20	1.083	0.62	253.00
18:00	42.41	43.26	43.99	39.17	41.58	40.38	2.42	0.30	1.057	0.47	29.00
4MM PINNED PLATE ABSORBER											
08:00	30.34	30.31	31.22	26.96	29.79	28.38	2.83	0.30	0.978	0.00	12.00
10:00	46.94	47.21	49.97	31.95	40.12	36.04	8.17	1.20	1.025	0.28	270.00
12:00	49.50	50.85	54.00	33.87	42.42	38.14	8.55	0.30	1.035	0.34	515.00
14:00	47.51	47.88	50.97	33.33	41.18	37.26	7.85	0.30	1.067	0.52	235.00
16:00	59.63	59.83	62.27	44.85	51.23	48.04	6.38	1.20	1.079	0.60	253.00
18:00	42.56	44.96	45.51	39.17	41.32	40.24	2.16	0.30	1.054	0.45	29.00
FLAT PLATE ABSORBER											
08:00	27.27	28.17	28.35	26.96	27.15	27.06	0.19	0.30	0.978	0.000	12.00
10:00	46.07	46.20	47.43	31.95	37.88	34.91	5.92	1.20	1.024	0.271	270.00
12:00	48.04	48.92	50.75	33.87	42.34	38.10	8.48	0.30	1.010	0.189	515.00
14:00	45.66	47.86	48.34	33.33	41.71	37.52	8.38	0.30	1.045	0.395	235.00
16:00	57.11	58.72	60.25	44.85	51.89	48.37	7.04	1.20	1.061	0.489	253.00
18:00	42.27	43.48	43.86	39.17	40.96	40.06	1.79	0.30	1.042	0.377	29.00

Table II.6 Analyzed data for 10° degree inclination angle

Time	Fluid Properties at Film Temperature							Thermal Properties								
	T _f (°C)	β	ρ(kg/m ³)	C _p (J/kgK)	ν (m ² /s)	k (W/m ² K)	Pr	T _A (°C)	\dot{m} (kg/s)	V _{out} (m/s)	Q̇(W)	h	Nu	Gr	Ra	Re
2MM STAGGERED PINNED PLATE ABSORBER																
08:00	26	3.34E-03	1.180	1007	1.571E-05	0.0256	0.7293	30.92	0.0126	0.318	8.00	51.76	247.19	1.11E+06	8.13E+05	2.47E+03
10:00	37	3.23E-03	1.138	1007	1.674E-05	0.0264	0.7263	68.90	0.0173	0.454	130.47	120.72	558.76	6.63E+06	4.82E+06	3.31E+03
12:00	44	3.16E-03	1.113	1007	1.740E-05	0.0267	0.7244	67.27	0.0218	0.583	377.69	474.96	2175.42	4.42E+06	3.20E+06	4.10E+03
14:00	28	3.33E-03	1.172	1007	1.590E-05	0.0257	0.7288	32.75	0.0094	0.239	20.53	118.32	561.82	1.22E+06	8.87E+05	1.83E+03
16:00	29	3.32E-03	1.168	1007	1.599E-05	0.0258	0.7258	33.72	0.0125	0.318	20.50	119.57	566.10	1.18E+06	8.59E+05	2.43E+03
18:00	26	3.35E-03	1.180	1007	1.571E-05	0.0256	0.7293	27.35	0.0067	0.168	0.20	3.26	15.58	4.46E+05	3.25E+05	1.31E+03
3MM STAGGERED PINNED PLATE ABSORBER																
08:00	26	3.34E-03	1.180	1007	1.571E-05	0.0256	0.7293	31.73	0.0147	0.371	3.41	18.08	86.36	1.36E+06	9.91E+05	2.89E+03
10:00	39	3.21E-03	1.131	1007	1.693E-05	0.0265	0.7258	71.03	0.0195	0.513	226.09	208.59	960.05	6.46E+06	4.69E+06	3.70E+03
12:00	41	3.18E-03	1.123	1007	1.712E-05	0.0267	0.7252	71.23	0.0193	0.513	233.42	229.77	1051.68	5.88E+06	4.27E+06	3.66E+03
14:00	28	3.33E-03	1.172	1007	1.590E-05	0.0257	0.7288	32.98	0.0188	0.477	45.04	253.65	1204.40	1.24E+06	9.07E+05	3.67E+03
16:00	29	3.31E-03	1.168	1007	1.599E-05	0.0258	0.7258	34.00	0.0125	0.318	26.78	155.23	734.94	1.19E+06	8.64E+05	2.43E+03
18:00	26	3.35E-03	1.180	1007	1.571E-05	0.0256	0.7293	27.36	0.0105	0.265	2.96	51.34	245.17	4.17E+05	3.04E+05	2.06E+03
4MM STAGGERED PINNED PLATE ABSORBER																
08:00	26	3.34E-03	1.180	1007	1.571E-05	0.0256	0.7293	31.60	0.0250	0.630	5.03	27.24	130.10	1.33E+06	9.72E+05	4.90E+03
10:00	37	3.23E-03	1.138	1007	1.674E-05	0.0264	0.7263	71.02	0.0217	0.569	165.26	143.62	664.73	7.06E+06	5.13E+06	4.15E+03
12:00	43	3.17E-03	1.116	1007	1.731E-05	0.0268	0.7247	68.50	0.0278	0.742	444.96	518.01	2357.91	4.83E+06	3.50E+06	5.24E+03
14:00	27	3.33E-03	1.176	1007	1.580E-05	0.0257	0.7290	32.59	0.0189	0.477	30.38	170.98	814.19	1.26E+06	9.20E+05	3.69E+03
16:00	28	3.32E-03	1.172	1007	1.590E-05	0.0257	0.7288	33.57	0.0206	0.524	12.06	65.48	310.90	1.29E+06	9.40E+05	4.03E+03
18:00	26	3.35E-03	1.180	1007	1.571E-05	0.0256	0.7293	27.44	0.0054	0.136	1.51	25.06	119.70	4.37E+05	3.18E+05	1.05E+03
FLAT PLATE ABSORBER																
08:00	26	3.34E-03	1.180	1007	1.571E-05	0.0256	0.7293	29.71	0.0142	0.359	0.29	2.31	11.03	8.97E+05	6.54E+05	2.79E+03
10:00	37	3.23E-03	1.138	1007	1.674E-05	0.0264	0.7263	62.42	0.0252	0.660	179.87	206.83	957.29	5.34E+06	3.88E+06	4.82E+03
12:00	39	3.20E-03	1.131	1007	1.693E-05	0.0265	0.7258	66.53	0.0166	0.436	139.27	151.54	697.47	5.47E+06	3.97E+06	3.15E+03
14:00	27	3.34E-03	1.176	1007	1.580E-05	0.0257	0.7290	30.44	0.0042	0.106	2.74	22.56	107.41	8.65E+05	6.30E+05	8.20E+02
16:00	28	3.32E-03	1.172	1007	1.590E-05	0.0257	0.7288	32.76	0.0125	0.318	1.89	11.54	54.80	1.15E+06	8.37E+05	2.45E+03
18:00	26	3.35E-03	1.180	1007	1.571E-05	0.0256	0.7293	26.42	0.0137	0.346	2.07	73.20	349.59	2.04E+05	1.49E+05	2.69E+03

Table II.7 Analyzed data for 30° degree inclination angle

Time	Fluid Properties at T film							Thermal Properties								
	T _r (°C)	β	ρ(kg/m ³)	C _p (J/kgK)	ν (m ² /s)	k (W/m ² K)	Pr	T _A (°C)	\dot{m}	V _{out} (m/s)	Q̇(W)	h	Nu	Gr	Ra	Re
2MM STAGGERED PINNED PLATE ABSORBER																
8:00	27	3.33E-03	1.176	1007	1.580E-05	0.02566	0.7290	33.10	0.0004	0.010	0.54	2.60	12.39	1.46E+06	1.07E+06	7.97E+01
10:00	37	3.22E-03	1.138	1007	1.674E-05	0.02640	0.7263	59.13	0.0200	0.523	225.55	310.03	1434.97	4.45E+06	3.23E+06	3.82E+03
12:00	41	3.19E-03	1.123	1007	1.712E-05	0.02669	0.7252	62.63	0.0174	0.461	207.30	280.84	1285.44	4.28E+06	3.10E+06	3.29E+03
14:00	39	3.21E-03	1.131	1007	1.693E-05	0.0265	0.7258	59.20	0.0212	0.557	228.53	336.56	1549.09	4.05E+06	2.94E+06	4.02E+03
16:00	28	3.32E-03	1.172	1007	1.590E-05	0.02573	0.7288	32.41	0.0048	0.122	6.75	49.33	234.22	9.57E+05	6.98E+05	9.40E+02
18:00	25	3.35E-03	1.184	1007	1.562E-05	0.02551	0.7296	26.38	0.0004	0.010	0.51	11.78	56.44	3.18E+05	2.32E+05	7.68E+01
3MM STAGGERED PINNED PLATE ABSORBER																
8:00	27	3.34E-03	1.176	1007	1.580E-05	0.02566	0.7290	34.03	0.0001	0.003	0.10	0.42	1.98	1.74E+06	1.27E+06	2.28E+01
10:00	38	3.22E-03	1.134	1007	1.683E-05	0.02647	0.7260	60.91	0.0164	0.430	186.66	237.56	1096.46	4.76E+06	3.45E+06	3.12E+03
12:00	40	3.19E-03	1.127	1007	1.702E-05	0.02662	0.7255	63.18	0.0191	0.505	218.99	286.47	1314.84	4.48E+06	3.25E+06	3.63E+03
14:00	38	3.21E-03	1.134	1007	1.683E-05	0.02647	0.7260	59.27	0.0192	0.504	179.87	254.97	1176.83	4.26E+06	3.09E+06	3.66E+03
16:00	28	3.32E-03	1.172	1007	1.590E-05	0.02573	0.7288	32.02	0.0034	0.085	3.32	25.46	120.87	9.13E+05	6.65E+05	6.57E+02
18:00	25	3.36E-03	1.184	1007	1.562E-05	0.02551	0.7296	26.20	0.0002	0.004	0.11	2.31	11.08	3.49E+05	2.55E+05	3.07E+01
4MM STAGGERED PINNED PLATE ABSORBER																
8:00	27	3.33E-03	1.176	1007	1.580E-05	0.02566	0.7290	33.09	0.0000	0.000	0.00	0.00	0.00	1.45E+06	1.05E+06	0.00E+00
10:00	37	3.22E-03	1.138	1007	1.674E-05	0.02640	0.7263	59.94	0.0146	0.382	164.99	218.70	1012.24	4.62E+06	3.35E+06	2.78E+03
12:00	40	3.19E-03	1.127	1007	1.702E-05	0.02662	0.7255	62.36	0.0194	0.511	204.49	272.08	1248.82	4.41E+06	3.20E+06	3.67E+03
14:00	38	3.21E-03	1.134	1007	1.683E-05	0.02647	0.7260	58.05	0.0103	0.270	98.79	149.66	690.76	3.98E+06	2.89E+06	1.96E+03
16:00	28	3.32E-03	1.172	1007	1.590E-05	0.02573	0.7288	31.85	0.0020	0.050	1.55	12.08	57.37	8.98E+05	6.54E+05	3.85E+02
18:00	25	3.36E-03	1.184	1007	1.562E-05	0.02551	0.7296	26.32	0.0001	0.002	0.09	1.93	9.25	3.28E+05	2.39E+05	1.54E+01
FLAT PLATE ABSORBER																
8:00	26	3.34E-03	1.180	1007	1.571E-05	0.02558	0.7293	31.21	0.0065	0.165	0.09	0.52	2.48	1.18E+06	8.62E+05	1.28E+03
10:00	36	3.24E-03	1.141	1007	1.664E-05	0.02632	0.7265	54.02	0.0198	0.516	149.66	242.25	1124.39	3.85E+06	2.80E+06	3.78E+03
12:00	38	3.22E-03	1.134	1007	1.683E-05	0.02647	0.7260	57.79	0.0209	0.549	130.11	194.08	895.79	4.05E+06	2.94E+06	3.99E+03
14:00	37	3.23E-03	1.138	1007	1.674E-05	0.02640	0.7263	54.57	0.0205	0.536	122.56	202.90	939.12	3.71E+06	2.69E+06	3.91E+03
16:00	28	3.33E-03	1.172	1007	1.590E-05	0.02573	0.7288	30.80	0.0133	0.337	0.68	6.47	30.70	7.37E+05	5.37E+05	2.59E+03
18:00	25	3.36E-03	1.184	1007	1.562E-05	0.02551	0.7296	25.88	0.0002	0.004	0.10	2.73	13.06	2.75E+05	2.01E+05	3.07E+01

Table II.8 Analyzed data for 50° degree inclination angle

Time	Fluid Properties at T film							Thermal Properties								
	T _f (°C)	β	ρ (kg/m ³)	C _p (J/kgK)	ν (m ² /s)	k (W/m ² K)	Pr	T _a (°C)	\dot{m} (kg/s)	V _{out} (m/s)	\dot{Q} (W)	h	Nu	Gr	Ra	Re
2MM STAGGERED PINNED PLATE ABSORBER																
08:00	28	3.33E-03	1.172	1007	1.590E-05	0.0257	0.7288	31.87	0.0100	0.255	25.18	178.51	847.61	9.89E+05	7.21E+05	1.96E+03
10:00	37	3.23E-03	1.138	1007	1.674E-05	0.0264	0.7263	56.36	0.0225	0.588	347.59	531.20	2458.62	4.01E+06	2.92E+06	4.29E+03
12:00	42	3.17E-03	1.120	1007	1.721E-05	0.0268	0.7249	69.81	0.0269	0.716	526.54	567.87	2591.82	5.29E+06	3.83E+06	5.08E+03
14:00	40	3.20E-03	1.127	1007	1.702E-05	0.02662	0.7255	60.29	0.0210	0.554	287.75	412.31	1892.45	4.11E+06	2.98E+06	3.98E+03
16:00	34	3.26E-03	1.149	1007	1.646E-05	0.0262	0.7271	45.67	0.0132	0.342	92.32	233.23	1088.65	2.54E+06	1.84E+06	2.54E+03
18:00	27	3.33E-03	1.176	1007	1.580E-05	0.0257	0.7290	29.16	0.0051	0.130	9.67	151.82	722.95	4.52E+05	3.30E+05	1.00E+03
3MM STAGGERED PINNED PLATE ABSORBER																
08:00	27	3.33E-03	1.176	1007	1.580E-05	0.0257	0.7290	31.60	0.0089	0.225	17.49	124.02	590.55	1.00E+06	7.30E+05	1.74E+03
10:00	36	3.23E-03	1.141	1007	1.664E-05	0.02632	0.7265	56.86	0.0204	0.532	284.94	409.45	1900.47	4.33E+06	3.14E+06	3.90E+03
12:00	41	3.18E-03	1.123	1007	1.712E-05	0.0267	0.7252	69.88	0.0244	0.647	435.77	454.97	2082.44	5.54E+06	4.02E+06	4.62E+03
14:00	39	3.20E-03	1.131	1007	1.693E-05	0.0265	0.7258	59.60	0.0197	0.518	261.32	383.04	1763.02	4.06E+06	2.95E+06	3.74E+03
16:00	34	3.26E-03	1.149	1007	1.646E-05	0.0262	0.7271	45.12	0.0128	0.332	87.23	229.24	1070.00	2.44E+06	1.77E+06	2.46E+03
18:00	27	3.33E-03	1.176	1007	1.580E-05	0.0257	0.7290	28.36	0.0045	0.115	6.06	131.51	626.25	3.27E+05	2.39E+05	8.88E+02
4MM STAGGERED PINNED PLATE ABSORBER																
08:00	28	3.33E-03	1.172	1007	1.590E-05	0.0257	0.7288	31.75	0.0084	0.214	18.40	129.29	613.90	9.98E+05	7.28E+05	1.64E+03
10:00	36	3.23E-03	1.141	1007	1.664E-05	0.02632	0.7265	56.79	0.0204	0.532	296.40	433.08	2010.11	4.25E+06	3.09E+06	3.90E+03
12:00	41	3.18E-03	1.123	1007	1.712E-05	0.0267	0.7252	69.66	0.0241	0.638	426.58	447.76	2049.46	5.51E+06	4.00E+06	4.55E+03
14:00	39	3.21E-03	1.131	1007	1.693E-05	0.0265	0.7258	61.08	0.0191	0.502	238.42	320.10	1473.29	4.44E+06	3.22E+06	3.63E+03
16:00	33	3.26E-03	1.153	1007	1.636E-05	0.0261	0.7274	45.21	0.0114	0.295	69.51	175.64	822.24	2.57E+06	1.87E+06	2.20E+03
18:00	27	3.33E-03	1.176	1007	1.580E-05	0.0257	0.7290	28.89	0.0049	0.124	8.86	158.51	754.83	3.97E+05	2.89E+05	9.57E+02
FLAT PLATE ABSORBER																
08:00	27	3.34E-03	1.176	1007	1.580E-05	0.0257	0.7290	30.65	0.0115	0.290	5.75	43.02	204.87	9.51E+05	6.93E+05	2.24E+03
10:00	35	3.25E-03	1.145	1007	1.655E-05	0.0263	0.7268	52.56	0.0228	0.592	269.46	458.69	2135.01	3.71E+06	2.69E+06	4.37E+03
12:00	39	3.20E-03	1.131	1007	1.693E-05	0.0265	0.7258	64.38	0.0278	0.731	376.61	446.08	2053.13	5.03E+06	3.65E+06	5.27E+03
14:00	38	3.22E-03	1.134	1007	1.683E-05	0.02647	0.7260	56.13	0.0353	0.925	362.98	589.99	2723.12	3.72E+06	2.70E+06	6.71E+03
16:00	33	3.27E-03	1.153	1007	1.636E-05	0.0261	0.7274	43.16	0.0198	0.511	95.92	276.12	1292.59	2.26E+06	1.64E+06	3.81E+03
18:00	27	3.34E-03	1.176	1007	1.580E-05	0.0257	0.7290	28.46	0.0129	0.327	10.19	174.17	829.39	4.16E+05	3.03E+05	2.53E+03

Table II.9 Analyzed data for 70° degree inclination angle

Time	Fluid Properties at T film							Thermal Properties								
	T _f (°C)	β	ρ(kg/m ³)	C _p (J/kg.K)	ν (m ² /s)	k (W/mK)	Pr	T _A (°C)	\dot{m} (kg/s)	V _{out} (m/s)	\dot{Q} (W)	h	Nu	Gr	Ra	Re
2MM STAGGERED PINNED PLATE ABSORBER																
8:00	27	3.33E-03	1.176	1007	1.580E-05	0.0257	0.7290	32.67	0.0001	0.002	0.20	1.09	5.21	1.31E+06	9.57E+05	1.52E+01
10:00	36	3.24E-03	1.141	1007	1.664E-05	0.02632	0.7265	51.45	0.0180	0.469	176.97	339.90	1577.64	3.24E+06	2.35E+06	3.45E+03
12:00	41	3.18E-03	1.123	1007	1.712E-05	0.0267	0.7252	65.82	0.0249	0.660	392.55	475.61	2176.92	4.77E+06	3.46E+06	4.71E+03
14:00	37	3.22E-03	1.138	1007	1.674E-05	0.0264	0.7263	54.13	0.0189	0.495	191.65	340.99	1578.26	3.44E+06	2.50E+06	3.61E+03
16:00	44	3.16E-03	1.113	1007	1.740E-05	0.0269	0.7244	53.58	0.0158	0.422	70.38	209.65	951.68	1.86E+06	1.35E+06	2.96E+03
18:00	33	3.27E-03	1.153	1007	1.636E-05	0.0261	0.7274	34.19	0.0017	0.045	1.46	30.00	140.45	3.17E+05	2.31E+05	3.37E+02
3MM STAGGERED PINNED PLATE ABSORBER																
8:00	27	3.34E-03	1.176	1007	1.580E-05	0.0257	0.7290	31.83	0.0000	0.000	0.00	0.00	0.00	1.21E+06	8.80E+05	0.00E+00
10:00	36	3.24E-03	1.141	1007	1.664E-05	0.02632	0.7265	51.83	0.0209	0.546	191.71	352.00	1633.78	3.39E+06	2.46E+06	4.01E+03
12:00	40	3.19E-03	1.127	1007	1.702E-05	0.02662	0.7255	67.80	0.0250	0.660	353.44	384.58	1765.18	5.39E+06	3.91E+06	4.74E+03
14:00	37	3.22E-03	1.138	1007	1.674E-05	0.0264	0.7263	54.46	0.0197	0.515	197.60	343.88	1591.61	3.52E+06	2.56E+06	3.76E+03
16:00	43	3.16E-03	1.116	1007	1.731E-05	0.0268	0.7247	53.69	0.0162	0.432	60.02	170.43	775.76	1.98E+06	1.43E+06	3.05E+03
18:00	32	3.27E-03	1.156	1007	1.627E-05	0.0260	0.7276	33.60	0.0029	0.074	0.22	5.20	24.43	2.74E+05	1.99E+05	5.53E+02
4MM STAGGERED PINNED PLATE ABSORBER																
8:00	27	3.33E-03	1.176	1007	1.580E-05	0.0257	0.7290	32.57	0.0000	0.000	0.00	0.00	0.00	1.32E+06	9.63E+05	0.00E+00
10:00	35	3.24E-03	1.145	1007	1.655E-05	0.0263	0.7268	51.91	0.0209	0.544	175.81	313.96	1461.35	3.53E+06	2.57E+06	4.02E+03
12:00	40	3.19E-03	1.127	1007	1.702E-05	0.02662	0.7255	65.52	0.0231	0.611	311.52	364.97	1675.14	5.01E+06	3.64E+06	4.38E+03
14:00	37	3.23E-03	1.138	1007	1.674E-05	0.0264	0.7263	53.45	0.0159	0.416	138.12	245.15	1134.66	3.46E+06	2.51E+06	3.04E+03
16:00	43	3.16E-03	1.116	1007	1.731E-05	0.0268	0.7247	51.85	0.0166	0.442	53.68	180.19	820.22	1.68E+06	1.21E+06	3.12E+03
18:00	33	3.27E-03	1.153	1007	1.636E-05	0.0261	0.7274	34.04	0.0064	0.165	5.33	121.41	568.35	2.85E+05	2.08E+05	1.23E+03
FLAT PLATE ABSORBER																
8:00	26	3.34E-03	1.180	1007	1.571E-05	0.0256	0.7293	30.65	0.0002	0.004	0.15	1.04	4.98	1.04E+06	7.57E+05	3.05E+01
10:00	34	3.26E-03	1.149	1007	1.646E-05	0.0262	0.7271	47.50	0.0196	0.507	109.97	240.10	1120.72	2.94E+06	2.13E+06	3.76E+03
12:00	38	3.21E-03	1.134	1007	1.683E-05	0.02647	0.7260	59.40	0.0278	0.729	281.60	400.37	1847.91	4.24E+06	3.08E+06	5.29E+03
14:00	36	3.23E-03	1.141	1007	1.664E-05	0.02632	0.7265	49.52	0.0205	0.534	170.20	389.04	1805.71	2.72E+06	1.97E+06	3.92E+03
16:00	42	3.17E-03	1.120	1007	1.721E-05	0.0268	0.7249	51.09	0.0177	0.471	39.39	136.14	621.35	1.65E+06	1.20E+06	3.35E+03
18:00	32	3.27E-03	1.156	1007	1.627E-05	0.0260	0.7276	33.74	0.0085	0.218	1.71	38.48	180.64	2.92E+05	2.13E+05	1.64E+03

Table II.10 Analyzed data for 90° degree inclination angle

Time	Fluid Properties at T film							Thermal Properties								
	T _r (°C)	β	ρ(kg/m ³)	C _p (J/kg.K)	v (m ² /s)	k (W/m.K)	Pr	T _A (°C)	ṁ(kg/s)	V _{out} (m/s)	Q̇(W)	h	Nu	Gr	Ra	Re
2MM STAGGERED PINNED PLATE ABSORBER																
8:00	28	3.33E-03	1.172	1007	1.590E-05	0.0257	0.7288	30.41	0.0000	0.000	0.00	0.00	0.00	6.29E+05	4.59E+05	0.00E+00
10:00	36	3.23E-03	1.141	1007	1.664E-05	0.02632	0.7265	49.48	0.0113	0.295	100.26	227.39	1055.42	2.74E+06	1.99E+06	2.16E+03
12:00	39	3.21E-03	1.131	1007	1.693E-05	0.0265	0.7258	53.47	0.0150	0.395	144.47	290.11	1335.28	2.97E+06	2.16E+06	2.85E+03
14:00	37	3.22E-03	1.138	1007	1.674E-05	0.0264	0.7263	50.53	0.0153	0.401	128.34	292.93	1355.83	2.68E+06	1.95E+06	2.92E+03
16:00	49	3.11E-03	1.095	1007	1.959E-05	0.0273	0.7231	62.35	0.0234	0.636	178.59	387.57	1735.98	1.99E+06	1.44E+06	3.97E+03
18:00	41	3.19E-03	1.123	1007	1.712E-05	0.0267	0.7252	45.37	0.0138	0.365	40.50	254.05	1162.82	9.24E+05	6.70E+05	2.61E+03
3MM STAGGERED PINNED PLATE ABSORBER																
8:00	28	3.33E-03	1.172	1007	1.590E-05	0.0257	0.7288	30.78	0.0000	0.000	0.00	0.00	0.00	7.25E+05	5.28E+05	0.00E+00
10:00	36	3.24E-03	1.141	1007	1.664E-05	0.02632	0.7265	50.47	0.0169	0.442	130.84	265.25	1231.15	3.07E+06	2.23E+06	3.24E+03
12:00	39	3.21E-03	1.131	1007	1.693E-05	0.0265	0.7258	54.15	0.0116	0.306	108.61	206.48	950.36	3.14E+06	2.28E+06	2.21E+03
14:00	38	3.22E-03	1.134	1007	1.683E-05	0.02647	0.7260	49.28	0.0155	0.407	146.66	387.98	1790.71	2.28E+06	1.66E+06	2.95E+03
16:00	49	3.11E-03	1.095	1007	1.959E-05	0.0273	0.7231	61.14	0.0228	0.619	190.95	468.81	2099.88	1.76E+06	1.27E+06	3.86E+03
18:00	40	3.19E-03	1.127	1007	1.702E-05	0.02662	0.7255	43.99	0.0176	0.465	42.89	352.71	1618.89	7.13E+05	5.18E+05	3.34E+03
4MM STAGGERED PINNED PLATE ABSORBER																
8:00	28	3.32E-03	1.172	1007	1.590E-05	0.0257	0.7288	31.22	0.0000	0.000	0.00	0.00	0.00	6.68E+05	4.86E+05	0.00E+00
10:00	36	3.24E-03	1.141	1007	1.664E-05	0.02632	0.7265	49.97	0.0106	0.277	87.34	186.53	865.78	2.91E+06	2.12E+06	2.03E+03
12:00	38	3.21E-03	1.134	1007	1.683E-05	0.02647	0.7260	54.00	0.0128	0.336	110.20	206.82	954.56	3.22E+06	2.34E+06	2.44E+03
14:00	37	3.22E-03	1.138	1007	1.674E-05	0.0264	0.7263	50.97	0.0200	0.524	158.56	344.08	1592.58	2.82E+06	2.05E+06	3.83E+03
16:00	48	3.11E-03	1.099	1007	1.779E-05	0.0272	0.7233	62.27	0.0220	0.595	141.23	295.46	1326.91	2.51E+06	1.81E+06	4.09E+03
18:00	40	3.19E-03	1.127	1007	1.702E-05	0.02662	0.7255	45.51	0.0170	0.448	36.81	208.24	955.77	1.04E+06	7.53E+05	3.21E+03
FLAT PLATE ABSORBER																
8:00	27	3.33E-03	1.176	1007	1.580E-05	0.0257	0.7290	28.35	0.0000	0.000	0.00	0.00	0.00	3.08E+05	2.24E+05	0.00E+00
10:00	35	3.25E-03	1.145	1007	1.655E-05	0.0263	0.7268	47.43	0.0104	0.271	62.17	147.90	688.40	2.65E+06	1.93E+06	2.00E+03
12:00	38	3.21E-03	1.134	1007	1.683E-05	0.02647	0.7260	50.75	0.0072	0.189	61.32	144.35	666.25	2.57E+06	1.86E+06	1.37E+03
14:00	38	3.22E-03	1.134	1007	1.683E-05	0.02647	0.7260	48.34	0.0150	0.395	126.94	349.00	1610.83	2.20E+06	1.60E+06	2.87E+03
16:00	48	3.11E-03	1.099	1007	1.779E-05	0.0272	0.7233	60.25	0.0181	0.489	127.98	320.54	1439.56	2.09E+06	1.51E+06	3.36E+03
18:00	40	3.19E-03	1.127	1007	1.702E-05	0.02662	0.7255	43.86	0.0143	0.377	25.72	201.66	925.59	7.49E+05	5.43E+05	2.71E+03